DYNAMIC BEHAVIOR OF HEATED CYLINDRICAL AND CONICAL SHELLS

By
CHUNG-LI SUN

A DISSERTATION PRESENTED TO THE GRADUATE COUNCIL OF
THE UNIVERSITY OF FLORIDA
IN PARTIAL FULFILLMENT OF THE REQUIREMENTS FOR THE
DEGREE OF DOCTOR OF PHILOSOPHY

UNIVERSITY OF FLORIDA
August, 1967

ACKNOWLEDGMENTS

The author wishes to express his hearty gratitude to Dr. S. Y. Lu, chairman of his supervisory committee, for his constant inspiration and guidance throughout the entire period of this study. He also wishes to express his sincere appreciation to Dr. W. A. Nash, Chairman, Department of Engineering Science and Mechanics. Dr. Nash not only encouraged him to carry out the present program, but also made the financial support available. He is grateful to Dr. I. K. Ebcioglu, professor of the Department of Engineering Science and Mechanics and Dr. R. G. Blake, professor of the Department of Mathematics, for their valuable encouragement and advice. He is indebted to Mrs. Mara Lea Hetherington, who carried out the typing work of this dissertation so carefully and nicely. Her friendly cooperation is much more than just considering her work as a job. Finally, he would like to take this opportunity to acknowledge the support received from the Computing Center of the University of Florida. Without its service, he can hardly imagine that the numerical part could have been finished.

The results presented in this dissertation were obtained in the course of a research, partly supported by the National Science Foundation Grant GP-943, and partly supported by the Florida Engineering and Industrial Experiment Station, College of Engineering, University of Florida.

TABLE OF CONTENTS

Page

ACKNOWLEDGMENTS ii

LIST OF TABLES v

LIST OF FIGURES vi

NOTATIONS viii

ABSTRACT xi

CHAPTER

1. INTRODUCTION 1

2. BASIC RELATIONS AND METHOD OF APPROACH 10

   2.1 Coordinate System 10

   2.2 Elastic Stress-Strain-Displacement and Moment-Curvature-Displacement Relations 12

   2.3 Energy Expressions 15

   2.4 Boundary Conditions and Initial Conditions 18

   2.5 Method of Approach 18

3. LINEAR SOLUTIONS 25

   3.1 Conical Shells 25

      3.1.1 Transformation of coordinates 25

      3.1.2 The prebuckling solution 26

      3.1.3 Considerations of dynamic stability during buckling 30

   3.2 Cylindrical Shells 31

      3.2.1 The prebuckling solution 32

      3.2.2 Considerations of dynamic stability during buckling 33

Page

3.3 Numerical Results and Discussions 34
    3.3.1 Influence of the force frequency 35
    3.3.2 Influence of the radius-length parameter 36
    3.3.3 Influence of the radius-thickness parameter 36
    3.3.4 Influence of the appex angle 37
    3.3.5 Comparison between the effect of a ramp-type temperature load and a Heavyside temperature load 37
4. NONLINEAR SOLUTIONS 46
4.1 Conical Shells 46
    4.1.1 Basic governing nonlinear differential equations 46
    4.1.2 Nonlinear vibrations 50
    4.1.3 Dynamic stability and response 51
4.2 Cylindrical Shells 59
    4.2.1 Basic governing nonlinear equations 59
    4.2.2 Nonlinear vibrations 60
    4.2.3 Dynamic stability and response 61
4.3 Numerical Results and Discussions 62
5. CONCLUSION 80
REFERENCES 82
APPENDIX I - FORMULATIONS OF THE CONICAL SHELL 86
APPENDIX II - FORMULATIONS OF THE CYLINDRICAL SHELL 89
APPENDIX III - FLOW DIAGRAM OF COMPUTER COMPUTATIONS 91
BIOGRAPHICAL SKETCH 92

LIST OF TABLES

Table Page

I. Conversion of Coefficients of the Linear Mathieu Differential Equation. 38

II. Conversion of Coefficients of the Nonlinear Mathieu Differential Equation. 58

LIST OF FIGURES

Figure Page

1. Coordinate Systems 11

2. Mathieu's Diagram of Conical Shell under Sinusoidal Temperature Loading with Three Frequencies $\Omega_1 = 0.3$, 1.0, 1.5 ($\bar{R}/H = 1$, $\alpha T_0 = 3.5 \times 10^{-4}$, $\omega = 0.77$, $\theta = 20^\circ$). 39

3. Mathieu's Diagram of Cylindrical Shell under Sinusoidal Temperature Loading with Three Frequencies, $\Omega_1 = 0.3, 1.0, 1.5$ ($R/L = 1$, $\alpha T_0 = 0.13 \times 10^{-4}$, $\omega_c = 0.99$). 40

4. Mathieu's Diagram of a Conical Shell under Sinusoidal Temperature Loading ($\Omega_1 = 1.5$, $\alpha T_0 = 3.5 \times 10^{-4}$). 41

5. Mathieu's Diagram of a Cylindrical Shell under Sinusoidal Temperature Loading ($\Omega_1 = 1.5$, $\alpha T_0 = 3.5 \times 10^{-4}$). 42

6. Mathieu's Diagram of a Conical Shell under Sinusoidal Temperature Loading ($\Omega_1 = 1.5$, $\alpha T_0 = 3.5 \times 10^{-4}$, $\theta = 20^\circ$). 43

7. Mathieu's Diagram of a Conical Shell under Ramp-Type and Heavyside Temperature Loadings ($\zeta_0 = 0.1$, $\theta = 20^\circ$, $T_1/(T_{cr})_{st} = 1$). 44

8. Mathieu's Diagram of a Cylindrical Shell under Ramp-Type and Heavyside Temperature Loadings ($L = 2R$, $T_1/(T_{cr}^{c})_{st} = 1$). 45

9. Amplitude-Frequency Diagram. 55

10. Jump Diagram. 56

11. Frequency Parameter Diagram of a Conical Shell ($\bar{R}/H = 0.5$, $\bar{R}/h = 500$, $\theta = 10^\circ$). 65

12. Critical Temperature Diagram of a Conical Shell under Sinusoidal Temperature Loading ($\bar{R}/H = 0.5$, $\bar{R}/h = 500$, $\theta = 10^\circ$, $\Omega_1^2 = 4\Omega_{mn}^2, 9\Omega_{mn}^2$). 66

13. Critical Temperature Diagram of a Conical Shell under Ramp-Type or Heavyside Temperature Loading ($\bar{R}/H = 0.5$, $\bar{R}/h = 500$, $\theta = 10^\circ$). 67

Figure Page

14. Temperature Parameter Diagram of a Conical Shell under Ramp-Type and Heavyside Temperature Loadings ($\bar{R}/H = 0.5$, $\bar{R}/h = 500$, $\theta = 10^\circ$, $t_o = \pi\bar{\tau}$, 0). 68

15. Nonlinear Spring Force Parameter Diagram of a Conical Shell ($\bar{R}/H = 0.5$, $\bar{R}/h = 500$, $\theta = 10^\circ$). 69

16. Frequency Parameter Diagram of a Cylindrical Shell ($R/L = 0.5$, $R/h = 500$). 70

17. Critical Temperature Diagram of a Cylindrical Shell under Sinusoidal Temperature Loading ($R/L = 0.5$, $R/h = 500$, $\Omega_1^2 = 4(\Omega_{mn}^c)^2$, $9(\Omega_{mn}^c)^2$). 71

18. Critical Temperature Diagram of a Cylindrical Shell under Ramp-Type or Heavyside Temperature Loading ($R/L = 0.5$, $R/h = 500$). 72

19. Temperature Parameter Diagram of a Cylindrical Shell under Ramp-Type and Heavyside Temperature Loadings ($R/L = 0.5$, $R/h = 500$, $t_o = \pi\bar{\tau}$, 0). 73

20. Nonlinear Spring Force Parameter Diagram of a Cylindrical Shell ($R/L = 0.5$, $R/h = 500$). 74

21. Nonlinear Free Vibration of a Conical Shell ($\bar{R}/H = 0.5$, $\bar{R}/h = 500$, $\theta = 10^\circ$). 75

22. Nonlinear Free Vibration of a Cylindrical Shell ($R/L = 0.5$, $R/h = 500$). 76

23. Amplitude-Frequency Diagram with Constant β . 77

24. Amplitude-Frequency Diagram with Constant μ . 78

25. Amplitude-Frequency Diagram of a Conical Shell ($\bar{R}/H = 0.5$, $\bar{R}/h = 500$, $\theta = 10^\circ$, $\alpha T_o = 6.6 \times 10^{-4}$, $\alpha T_1 = 6.6 \times 10^{-4}$, $\Omega_1 = 3\Omega_{mn}$, $t_o = 0$, $\pi\bar{\tau}$). 79

NOTATIONS

A, B	Coefficients of the first quadratic form.
A_1, A_2, A_3	Time-dependent amplitudes of u'' (after buckling).
$\bar{A}_1, \bar{A}_2, \bar{A}_3$	Nondimensional amplitudes, $\bar{A}_1 = A_1/h$, $\bar{A}_2 = A_2/h$, $\bar{A}_3 = A_3/h$.
A_{1c}, A_{2c}, A_{3c}	Time-dependent amplitudes of u''_c (after buckling).
$\bar{A}_{1c}, \bar{A}_{2c}, \bar{A}_{3c}$	Nondimensional amplitudes, $\bar{A}_{1c} = A_{1c}/h$, $\bar{A}_{2c} = A_{2c}/h$, $\bar{A}_{3c} = A_{3c}/h$.
B_1, B_2	Time-dependent amplitudes of v'' (after buckling).
$\bar{B}_1, \bar{B}_2$	Nondimensional amplitudes, $\bar{B}_1 = B_1/h$, $\bar{B}_2 = B_2/h$.
B_{1c}, B_{2c}	Time-dependent amplitudes of v''_c (after buckling).
$\bar{B}_{1c}, \bar{B}_{2c}$	Nondimensional amplitudes, $\bar{B}_{1c} = B_{1c}/h$, $\bar{B}_{2c} = B_{2c}/h$.
C_1	Time-dependent amplitude of w'' (after buckling).
$\bar{C}_1$	Nondimensional amplitude, $\bar{C}_1 = C_1/h$.
C_{1c}	Time-dependent amplitude of w''_c (after buckling).
$\bar{C}_{1c}$	Nondimensional amplitude, $\bar{C}_{1c} = C_{1c}/h$.
D	Bending rigidity $= Eh^3/12(1-\nu^2)$.
E	Young's modulus.
H	Height of conical shell (See Fig. 1).
L	Length of cylindrical shell.
$M_x, M_\phi, M_{x\phi}$	Bending and twisting moments.
$M'_x, M'_\phi, M'_{x\phi}$	Prebuckling bending and twisting moments.
$M''_x, M''_\phi, M''_{x\phi}$	Additional bending and twisting moments during and after buckling.
Q'_u, Q'_w	Time-dependent amplitudes of u', w'.

Q'_{uc}, Q'_{wc}	Time-dependent amplitudes of u'_c, w'_c.
Q''_u, Q''_v, Q''_w	Time-dependent amplitudes of u'', v'', w'' (during buckling).
$Q''_{uc}, Q''_{vc}, Q''_{wc}$	Time-dependent amplitudes of u''_c, v''_c, w''_c (during buckling).
R, R_1, R_2	Radii defined in Figure 1.
$\bar{R}$	Mean radius $=(R_1+R_2)/2$.
T	Temperature function.
T_0, T_1	Constant temperature gradients.
$(T_{cr})_{st}$	Static buckling temperature.
U, V	Strain energy and kinetic energy, respectively.
U_m, U_b, U_T	Membrane, bending and thermal strain energies.
X, Y, Z	Cartesian coordinates.
a_1	Amplitude of nonlinear free vibration.
b_1, c_1	Amplitudes of nonlinear response of deformation.
h	Thickness of the shell.
k_x, k_ϕ	Curvatures of the shell.
m	Number of half waves in longitudinal direction.
n	Number of waves in circumferential direction.
$r_x^{-1}, r_\phi^{-1}, r_{x\phi}^{-1}$	Changes of curvature.
t	Time.
u, v, w	Displacement components.
u', w'	Prebuckling displacement components.
u'', v'', w''	Buckling or post-buckling displacement components.
x, ϕ	Coordinates of the middle surface.
ζ, ψ	Transformed coordinates of conical shells.
α	Thermal expansion coefficient.
β	Nonlinear spring force parameter in Equation (4.19).
δ	Variational symbol.

$\epsilon_x, \epsilon_\phi, \epsilon_{x\phi}$	Strain components ($\epsilon_x = \epsilon_x' + \epsilon_x'', \cdots$).
$\epsilon_x', \epsilon_\phi', \epsilon_{x\phi}'$	Linear strain components.
$\epsilon_x'', \epsilon_\phi'', \epsilon_{x\phi}''$	Nonlinear strain components.
η	Nonlinear spring force parameter of conical shells.
η_c	Nonlinear spring force parameter of cylindrical shells.
θ	Semivertex angle.
λ	$= (1-\nu)/2$.
μ	Force parameter in Equation (4.19).
ν	Poisson's ratio.
ξ	Frequency parameter defined as $\frac{\bar{\Omega}}{\Omega_{mn}}$.
ρ	Mass density.
$\sigma_x, \sigma_\phi, \sigma_{x\phi}$	Stress components.
$\sigma_x', \sigma_\phi', \sigma_{x\phi}'$	Prebuckling thermal stress components.
$\sigma_x'', \sigma_\phi'', \sigma_{x\phi}''$	Additional stress components during and after buckling.
τ	Nondimensional time $\tau = \left[\frac{E}{\rho R_1^2 (1-\nu^2)}\right]^{\frac{1}{2}} t$ or $\tau = \left[\frac{E}{\rho R^2 (1-\nu^2)}\right]^{\frac{1}{2}} t$.
ω	Natural frequency of shell.
ω_1, Ω_1	Temperature frequencies.
Ω_{mn}	Frequency parameter of shells.
$\bar{\Omega}$	A defined frequency in Equation (4.19).
Ω	Frequency of nonlinear free vibration.

Subscripts

c	Referred to the case of cylindrical shell.
h	Term pertaining to Heavyside temperature.
r	Term pertaining to ramp-type temperature.
S	Term pertaining to sinusoidal temperature.

Superscripts

c	Referred to the case of cylindrical shell.

Abstract of Dissertation Presented to the Graduate Council
in Partial Fulfillment of the Requirements for the Degree of
Doctor of Philosophy

DYNAMIC BEHAVIOR OF HEATED CYLINDRICAL AND CONICAL SHELLS

By

Chung-li Sun

August, 1967

Chairman: Dr. S. Y. Lu

Major Department: Engineering Science and Mechanics

The present analysis is to study the elastic, dynamic stability and response of conical and cylindrical shells subjected to time-dependent heating. Two phases of the problem were treated. First, a linear shallow shell theory was used. The shells become dynamically unstable when the normal displacement component due to thermal stresses increases unboundedly with time. Second, a nonlinear shallow shell theory has been adopted. The post-buckling amplitude-frequency relationship shows that the solution originating at the upper boundary of the instability region is always unstable, while the solution originating at the lower boundary of the instability region is always stable.

Two kinds of temperature change with respect to time were considered. In one case, the temperature change is sinusoidal, and in the other case, the temperature function is a ramp-type. The shells are simply supported and completely restricted at both ends. The Hamilton principle has been used for both the linear and nonlinear cases. The final equation in both cases is of the Mathieu type. The linear Mathieu differential equation was used to study the characteristics of the dynamic stability of the shells, and the nonlinear Mathieu differential equation was used to establish the amplitude-frequency diagram, so that the stable and unstable solutions were thus determined.

CHAPTER 1

INTRODUCTION

In recent years, owing to the rapid development of structural engineering, a new field entitled dynamic stability of elastic plates and shells has been intensively cultivated. The theory used in this field is generated from the study of stability of elastic systems under loads varying with time. In the analysis of dynamic stability of deformable bodies, the influences of inertia must be taken into consideration, and the system becomes dynamically unstable when the amplitudes of the vibrations increase unboundedly with time. Thus, the theory of dynamic stability of elastic systems can be defined as the study of vibrations induced by pulsating or impact loadings which are parametric with respect to certain displacement components.

This point of view can be illustrated by considering a rod compressed by a time-dependent force. If a straight rod is subjected to a periodic longitudinal load and if the amplitude of the load is less than that of the static buckling value, then, in general, the rod experiences only longitudinal vibrations. However, it has been known that for certain relationships between the force frequency and the natural frequency of transverse vibration a straight rod becomes unstable, and transverse vibrations occur. The amplitude of this vibration increases rapidly to large values. Such a phenomenon is called parametric resonance. The relationship of the frequencies at such a resonance differs from the frequency relationship for the ordinary forced vibration resonance. For sufficiently small values of the longitudinal force, this relationship is that the force frequency is equal to twice the value of natural frequency of the rod.

Similarly, periodic forces acting in the middle plane of a thin plate or shell can excite intensive transverse vibrations under certain conditions.

Another example is when a periodic loading is applied symmetrically with respect to an arch. It causes not only symmetrical vibrations, but sometimes can excite asymmetrical vibrations of very large amplitude.

In general, whenever there is a special kind of static loading which causes a loss of static stability, the vibrational loading of the same type will cause a loss of dynamic stability. Such a loading is characterized by the fact that it is contained as a parameter in the equation of motion. Therefore, it is called a parametric loading. This term is more appropriate because it indicates the relation to the phenomenon of parametric resonance.

The general concept stated above has been discussed by Ziegler [1] and Bolotin [2]. In the latter reference, the general theory of the dynamic stability of elastic systems is formulated, and examples for the cases of rods, beams, frames and plates under the periodic loading have been given. Linear problems of the circular cylindrical shell under a uniformly distributed radial periodical loading as well as a compressive periodical loading, and spherical shells subjected to a radial periodical loading uniformly distributed over the surface have been discussed also in reference [2].

A correlated problem to the problem of dynamic stability is the dynamic buckling. An elastic structure under any time-dependent loading may cause a finite jump of the deflection at certain value of the loading. This value is defined as the dynamic buckling load. For structures with large initial imperfections, such a jump will not happen. However, there would be a point of inflection on the deflection-loading curve, and the value of the loading at this point is considered to be the dynamic buckling load. A general criterion for dynamic buckling of elastic structures which are sensitive to initial imperfections, and some estimates for the dynamic buckling strengths of such structures subjected to various loading histories can be found in the paper of Budiansky [3].

The study of the problem of dynamic stability began in the early days of this century. In 1924, Beliaev [4] examined a problem of a hinged straight rod under axial loading. Later in 1935, Krylov and Bogoliubov [5] studied the same problem with arbitrary support conditions by applying the Galerkin method. In this part of the world, Lubkin and Stoker [6] first investigated this kind of problem in 1943, by analyzing the stability of columns and strings under periodically varying forces. Hoff [7], in 1954, examined the stability of bars with initial imperfection under dynamic loading by a compressing force.

In recent years, several authors studied the linear problems of dynamic stability of shells in further detail. Wood and Koval [8], in 1963, explored some experimental and analytical results of the collapse of thin-walled cylindrical shells with the initial imperfection under dead weight axial compression and axisymmetric transient and oscillatory hydrostatic pressures. An eighth order partial differential equation of the Donnell type [9] has been solved by assuming a double Fourier series for the solution to the normal displacement. The resulting second order differential equation of the coefficients of the displacement function with respect to time was discussed on its stability under the step-pressure or sinusoidal pressure. In the same year, Yao [10] studied the dynamic stability bounds for complete cylindrical shells under various combinations of static and periodic radial as well as axial loads. The solutions were determined numerically by means of properties of the Mathieu functions. Goodier and McIvor [11], in 1964, considered the surface of a thin-walled cylinder subjected to impulsive pressure. They assumed the form of the normal displacement and substituted it into the formulated Lagrange equation of motion. The stable and unstable modes of the normal displacement were discussed through the obtained Mathieu equation. In 1966, Bieniek, Fan and Lackman [12] introduced a perturbation method to solve the same problem under ramp-type pressure and sinusoidal pressure. The result of the ramp-type pressure agrees with that in reference [11].

A nonlinear problem of dynamic stability of spherical shell was investigated in 1958 by Bolotin [13]. In this reference, the unsymmetric character of the nonlinearity on a curved panel reveals the essential difference in the behavior of a plate and a curved panel for parametric excitation. In the same year, Vol'mir [14] by using the Galerkin method and the method of numerical integration solved the problem of dynamic stability of a cylindrical panel with initial imperfection subjected to axial compression. In 1959, Agamirov and Vol'mir [15] used the same approximate technique as used in reference [14] to treat the same problem of a complete thin cylinder under a linearly increased time-dependent hydrostatic pressure. In both papers, the solution to the transverse displacement is assumed to the first degree of approximation, and a second order nonlinear differential equation of the time-dependent amplitude of the normal displacement was thus obtained. After this differential equation was numerically integrated, the critical conditions were depicted by the characteristics of the response curve. In 1961, Mishenkov [16] considered a shallow cylindrical panel under axial periodical compression. The Galerkin method was applied again by representing the normal displacement by the first term of a double Fourier series with time-dependent coefficient. A nonlinear differential equation of the second order with periodic coefficient was finally obtained, and periodic solutions to this equation near principal resonance were solved. The stability was thereupon investigated. In 1962, Cummings [17] examined both the cylindrical panel and the complete thin cylindrical shell under different forms of radial pressure. Although the investigation was interested mainly in the problem of vibration and response, the characteristics of loss of stability in a linear sense were also mentioned. In 1964, Ho and Nash [18] discussed the dynamic instability of thin shallow spherical shells under uniformly distributed impulsive loadings including an impulsive function, a step-function and a linear function of time. They used the Galerkin method as well as a dynamic stability theory to establish their solutions. The same techniques were then extended to the solution of complete spherical shells. In 1965, Wilder and Nash [19] investigated the response of a truncated conical shell subjected to the dynamic axial force. After first applying the variational principle to find out the nonlinear differential equation of the second order with respect to time, the Runge-Kutta numerical integration method was adopted to trace out the nonlinear response. All papers reviewed above followed the important simplification suggested by Reissner [20] in 1955, that the tangential inertia terms for thin-walled surface structures may be omitted with negligible errors.

Although the study of dynamic stability of cylindrical shells, by using both linear and nonlinear shallow shell theories, has been developed in such a broad scope, the parallel study of a conical shell still remains in a comparatively primitive stage. Moreover, similar problems dealing with a temperature loading are even less discussed. Only a few problems of the linear dynamic response, and certain problems of the static stability of beams, plates and shells under temperature loadings are listed. Boley [21] first treated the problem of thermally induced vibrations of beams in 1956. In this paper, he introduced a thermal moment in the beam equation by applying a sudden heat input to the upper surface of the beam uniformly distributed along its span. The ratio of the dynamic response, obtained by solving this equation, and the corresponding quasistatic deflection was plotted against a governing nondimensional time-ratio parameter. From this curve, Boley concluded that the maximum deflection under the dynamic effect is twice larger than that calculated through a quasistatic process. In 1957, Boley and Barber [22] extended the same problem to a plate, and drew out an analogous conclusion. Later in 1966, Kraus [23] investigated the same problem for spherical shells by use of a model expansion procedure. In 1967, Lu and Sun [24] examined this problem for truncated conical shells through a variational method. The significance of dynamic effects on deflection are evident in these references [21-24].

Hoff [25], in 1957, solved the thermal buckling problem of hinged thin cylindrical shells subjected to uniform surface temperature loading. He used the Donnell equation and concluded that the elastic thermal buckling is unlikely to occur except when the shell is very thin. In 1962, Sunakawa [26] studied the same problem for a clamped thin cylinder and found that the shell will buckle at a lower temperature than that for simply supported ends. In 1959, Huang and Van Der Maas [27] worked out the buckling problem of heated and simply supported plates with the Von Kármánn large deflection theory and Rayleigh-Ritz's method. Solution forms of the three components of displacement were chosen to be the first term of a double trigonometric series. For the two inplane displacement components, linear terms were added to justify the boundary conditions. In 1960, Boley [28] wrote a book on thermal stress analysis, in which both basic theories and applications to rods, beams, plates and shells are presented. In 1964, Hoff, Chao and Madsen [29] used the Donnell equation to analyze the buckling problem of a thin-walled cylindrical shell heated along an axial strip. In this report, solutions for heated and unheated regions were obtained separately, then coupled together through continuity of boundary conditions. Both symmetric and anti-symmetric bucklings were discussed. The conclusion is that the critical value of the compressive axial stress is found to be equal to the critical stress of the same circular cylindrical shell when subjected to uniform axial compression if the band is not extremely narrow. Otherwise, the critical stress will be higher.

The proposition of this dissertation consists of two parts. In the first part, a linear theory of shallow shells is adopted. Some qualitative characteristics of the dynamic stability of thin cylindrical and conical shells related to the induced time-dependent thermal loading, the geometry of the shells and the mode number of the normal displacement are investigated. In the second part, a nonlinear theory of shallow shells is followed. The post-buckling thermal response-frequency relationship was examined so that the stable and unstable region could be defined through the "jump" phenomenon.

The shells under consideration are assumed thin and of constant thickness. Two kinds of temperature change with respect to time were considered. In one case, the temperature gradient is sinusoidal, while in the other case, the temperature function is a ramp-type. The shells are simply supported and completely restricted at both ends. The Hamilton principle was applied to obtain the differential equations for the generalized coordinates. The problem was treated in two steps, of which the first is prior to buckling and the second is during buckling for the linear case and after buckling for the nonlinear case. The prebuckling relations are used to find the thermal stresses. The final differential equation for the linear case assumes the Mathieu type, and for the nonlinear case assumes the type of a second order nonlinear differential equation with variable coefficient. This nonlinear differential equation is of the same form as that of a nonlinear dynamic stability problem of a plate under axial periodic loadings [2]. The quadratic nonlinearity which shows up in the final differential equation of a curved panel is missing in the present case because of the completeness of the geometry of the shell along the circumferential direction.

In the linear case, the region of stability at various normal displacement modes has been studied. The behavior of stability depends upon the temperature function as well as the geometry of shells. In the nonlinear case, the force is always a type of hard spring force [30] for the present boundary conditions. The solutions originating at the lower boundary are therefore always stable while those originating at the upper boundary are always unstable.

CHAPTER 2

BASIC RELATIONS AND METHOD OF APPROACH

2.1 Coordinate System

The coordinate system chosen for a conical shell on its middle surface is (x,ϕ) as shown in Figure 1. This coordinate system assumes the geometric orthogonality of the shell. The transformations between this set of coordinates and the Cartesian coordinates (X, Y, Z) according to Figure 1 are given as follows

$$X = x \sin\theta \cos\phi , \quad Y = x \sin\theta \sin\phi , \quad Z = x \cos\theta \tag{2.1}$$

Substituting the above expressions into the relation

$$\vec{x} = X\vec{i} + Y\vec{j} + Z\vec{k}$$

and calculating the values of

$$A^2 = \frac{\partial \vec{x}}{\partial x} \cdot \frac{\partial \vec{x}}{\partial x} , \qquad B^2 = \frac{\partial \vec{x}}{\partial \phi} \cdot \frac{\partial \vec{x}}{\partial \phi}$$

one can immediately obtain the scale factors

$$A = 1 , \qquad B = x \sin\theta \tag{2.2}$$

For the limiting case as $x \to \infty$ and $\theta \to o$, i.e., for the case of circular cylindrical shell

$$A = 1 , \qquad B = R_1 = R_2 = R \tag{2.3}$$

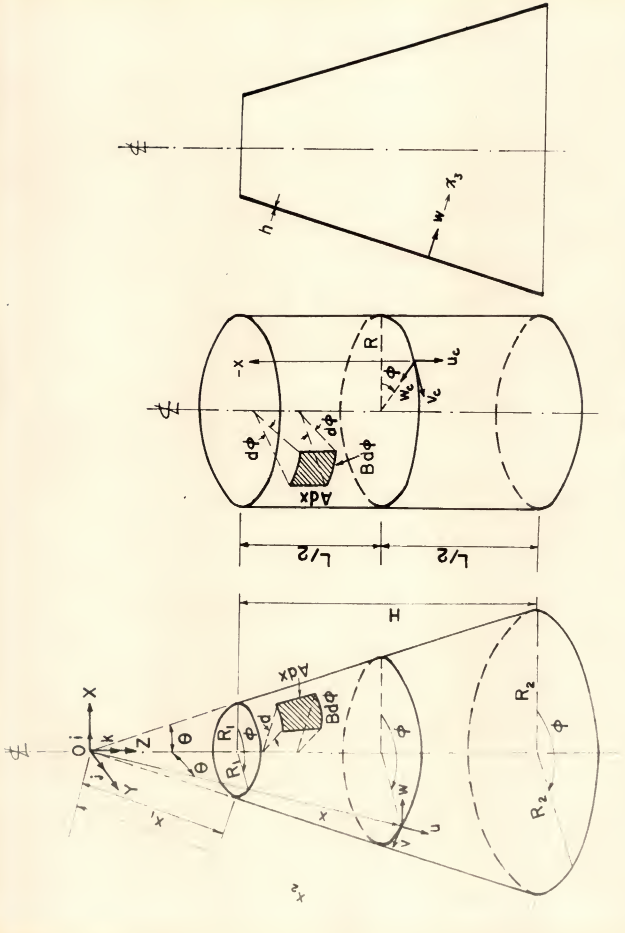
X
O
i
k
j
Y
Z
θ
θ
R1
R1
φ
x
x'
Adx
Bdφ
dφ
φ
u
v
w
R2
R2
φ
H
x2
L/2
L/2
-x
R
uc
vc
wc
φ
dφ
dφ
Bdφ
Adx
h
w
λ3

[illegible]

Also from Figure 1, one can easily observe that the principal curvature along χ and ϕ directions are

$$k_{\chi} = 0, \qquad k_{\phi} = (\chi \tan\theta)^{-1} \tag{2.4}$$

For a cylindrical shell

$$k_{\chi} = 0, \qquad k_{\phi} = R^{-1} \tag{2.5}$$

2.2 Elastic Stress-Strain-Displacement and Moment-Curvature-Displacement Relations

In the present investigation, the following basic assumptions are made

(1) Elements normal to the unstrained middle surface of the shell remain normal to the strained middle surface.

(2) The material obeys Hooke's law.

(3) In the nonlinear analysis, only normal displacement is assumed large.

Based upon the above assumptions, the strain-displacement relations to the middle surface of the shell under consideration are [31]

$$\epsilon_{\chi} = \frac{\partial u}{\partial \chi} + \frac{1}{2}\left(\frac{\partial w}{\partial \chi}\right)^2 \tag{2.6a}$$

$$\epsilon_{\phi} = \frac{1}{B}\frac{\partial v}{\partial \phi} + \frac{u}{B}\frac{\partial B}{\partial \chi} - k_{\phi} w + \frac{1}{2}\left(\frac{1}{B}\frac{\partial w}{\partial \phi}\right)^2 \tag{2.6b}$$

$$\epsilon_{\chi\phi} = \epsilon_{\phi\chi} = \frac{1}{2}\left\{\frac{\partial v}{\partial \chi} + \frac{1}{B}\frac{\partial u}{\partial \phi} - \frac{v}{B}\frac{\partial B}{\partial \chi} + \frac{1}{B}\frac{\partial w}{\partial \chi}\frac{\partial w}{\partial \phi}\right\} \tag{2.6c}$$

The stress-strain-displacement relations are [31]

$$\begin{aligned}\sigma_x &= \frac{E}{1-\nu^2}(\epsilon_x + \nu\epsilon_\phi) - \frac{E\alpha T}{1-\nu} \\ &= \frac{E}{1-\nu^2}\Big[\frac{\partial u}{\partial x} + \frac{1}{2}\Big(\frac{\partial w}{\partial x}\Big)^2 + \nu\Big(\frac{1}{B}\frac{\partial v}{\partial \phi} + \frac{u}{B}\frac{\partial B}{\partial x} - \\ &\qquad - k_\phi w + \frac{1}{2}\Big(\frac{1}{B}\frac{\partial w}{\partial \phi}\Big)^2\Big] - \frac{E\alpha T}{1-\nu}\end{aligned} \qquad (2.7a)$$

$$\begin{aligned}\sigma_\phi &= \frac{E}{1-\nu^2}(\epsilon_\phi + \nu\epsilon_x) - \frac{E\alpha T}{1-\nu} \\ &= \frac{E}{1-\nu^2}\Big[\frac{1}{B}\frac{\partial v}{\partial \phi} + \frac{u}{B}\frac{\partial B}{\partial x} - k_\phi w + \frac{1}{2}\Big(\frac{1}{B}\frac{\partial w}{\partial \phi}\Big)^2 + \\ &\qquad + \nu\Big(\frac{\partial u}{\partial x} + \frac{1}{2}\Big(\frac{\partial w}{\partial x}\Big)^2\Big)\Big] - \frac{E\alpha T}{1-\nu}\end{aligned} \qquad (2.7b)$$

$$\begin{aligned}\sigma_{x\phi} = \sigma_{\phi x} &= \frac{E}{1+\nu}\epsilon_{x\phi} \\ &= \frac{E}{2(1+\nu)}\Big(\frac{\partial v}{\partial x} + \frac{1}{B}\frac{\partial u}{\partial \phi} - \frac{v}{B}\frac{\partial B}{\partial x} + \frac{1}{B}\frac{\partial w}{\partial x}\frac{\partial w}{\partial \phi}\Big)\end{aligned} \qquad (2.7c)$$

The curvature-displacement relations are

$$(r_x)^{-1} = -\frac{\partial^2 w}{\partial x^2} \qquad (2.8a)$$

$$(r_\phi)^{-1} = -\frac{1}{B^2}\frac{\partial^2 w}{\partial \phi^2} - \frac{1}{B}\frac{\partial B}{\partial x}\frac{\partial w}{\partial x} \qquad (2.8b)$$

$$(r_{x\phi})^{-1} = (r_{\phi x})^{-1} = \frac{1}{B^2}\frac{\partial w}{\partial \phi}\frac{\partial B}{\partial x} - \frac{1}{B}\frac{\partial^2 w}{\partial x \partial \phi} \qquad (2.8c)$$

The moment-curvature-displacement relations are

$$M_x = D[(r_x)^{-1} + \nu(r_\phi)^{-1}]$$

$$= -D\left[\frac{\partial^2 w}{\partial x^2} + \nu\left(\frac{1}{B^2}\frac{\partial^2 w}{\partial \phi^2} + \frac{1}{B}\frac{\partial B}{\partial x}\frac{\partial w}{\partial x}\right)\right) \right] \tag{2.9a}$$

$$M_\phi = D[(r_\phi)^{-1} + \nu(r_x)^{-1}]$$

$$= -D\left[\frac{1}{B^2}\frac{\partial^2 w}{\partial \phi^2} + \frac{1}{B}\frac{\partial B}{\partial x}\frac{\partial w}{\partial x} + \nu\frac{\partial^2 w}{\partial x^2}\right] \tag{2.9b}$$

$$M_{x\phi} = M_{\phi x} = D(1-\nu)(r_{x\phi})^{-1}$$

$$= D(1-\nu)\left[\frac{1}{B^2}\frac{\partial w}{\partial \phi}\frac{\partial B}{\partial x} - \frac{1}{B}\frac{\partial^2 w}{\partial x \partial \phi}\right] \tag{2.9c}$$

In the above expressions, u, v, w are the displacement components at an arbitrary point on the middle surface of the shell and are measured along x, ϕ and normal directions, respectively (Fig. 1). The notations $\epsilon_x, \epsilon_\phi, \epsilon_{x\phi}$ and $\sigma_x, \sigma_\phi, \sigma_{x\phi}$ are the normal and shearing strains and stresses to the middle surface; M_x, M_ϕ and $M_{x\phi}$ are the bending and twisting moments, while $(r_x)^{-1}, (r_\phi)^{-1}, (r_{x\phi})^{-1}$ represent the changes of curvature. In this dissertation, E assumes Young's modulus, ν is Poisson's ratio, α represents the linear thermal expansional coefficient and $T = T(x, \phi, x_3, t)$ is a temperature function in which x_3 is the coordinate along the normal direction, and t is time. $D = \frac{Eh^3}{12(1-\nu^2)}$, in which h denotes the thickness of the shell.

2.3 Energy Expressions

Referring to the middle surface of the shell, the strain energy U can be considered as the sum of three parts [31], i.e.,

$$U = U_m + U_b + U_T$$

where U_m, U_b, U_T represent the membrane, bending and thermal energy, respectively. The expressions of these parts of energy in terms of strains and changes of curvature and finally in terms of displacements can be written as follows [31]

$$\begin{aligned} U_m &= \frac{D'}{2}\iint_S [\, \epsilon_x^2 + \epsilon_\phi^2 + 2\nu\epsilon_x\epsilon_\phi + 2(1-\nu)\epsilon_{x\phi}^2]\, B\, dx\, d\phi \\ &= \frac{D'}{2}\iint_S \{ [\, u_{,x} + \frac{1}{2}(w_{,x})^2]^2 + [\frac{1}{B}v_{,\phi} + \frac{u}{B}B_{,x} - k_\phi w + \\ &\quad + \frac{1}{2}(\frac{1}{B}w_{,\phi})^2]^2 + 2\nu[\, u_{,x} + \frac{1}{2}(w_{,x})^2][\frac{v_{,\phi}}{B} + \frac{u}{B}B_{,x} - \\ &\quad - k_\phi w + \frac{1}{2}(\frac{1}{B}w_{,\phi})^2] + \frac{1}{2}(1-\nu)[\, v_{,x} + \frac{1}{B}u_{,\phi} - \frac{v}{B}B_{,x} + \\ &\quad + \frac{1}{B}w_{,x}w_{,\phi}]^2 \}\, B\, dx\, d\phi \end{aligned} \tag{2.10}$$

$$\begin{aligned} U_b &= \frac{D}{2}\iint_S [\, (r_x^{-1})^2 + (r_\phi^{-1})^2 + 2\nu(r_x^{-1})(r_\phi^{-1}) + 2(1-\nu)(r_{x\phi}^{-1})^2]\, B\, dx\, d\phi \\ &= \frac{D}{2}\iint_S [\, (w_{,xx})^2 + (\frac{1}{B^2}w_{,\phi\phi} + \frac{1}{B}B_{,x}w_{,x})^2 + \\ &\quad + 2\nu w_{,xx}(\frac{1}{B^2}w_{,\phi\phi} + \frac{1}{B}B_{,x}w_{,x}) + \\ &\quad + \frac{1}{2}(1-\nu)(\frac{2}{B}w_{,x\phi} - \frac{2}{B^2}B_{,x}w_{,\phi})^2]\, B\, dx\, d\phi \end{aligned} \tag{2.11}$$

$$
\begin{aligned}
U_T &= -\frac{E}{1-\nu}\iint_S \left[(\epsilon_x+\epsilon_\phi)\bar{T} + (r_x^{-1}+r_\phi^{-1}) M_T \right] B\,dx\,d\phi \\
&= -\frac{E}{1-\nu}\iint_S \Big\{ \Big[u_{,x} + \frac{1}{2}(w_{,x})^2 + \frac{1}{B}v_{,\phi} + \frac{u}{B}B_{,x} - k_\phi w + \\
&\qquad + \frac{1}{2}\left(\frac{1}{B}w_{,\phi}\right)^2 \Big]\bar{T} + \Big[w_{,xx} + \frac{1}{B^2}w_{,\phi\phi} + \\
&\qquad + \frac{1}{B}B_{,x}w_{,x} \Big] M_T \Big\} B\,dx\,d\phi \qquad (2.12)
\end{aligned}
$$

where the integral is over the total middle surface S . The notations $\bar{T}$ and M_T are defined by the integrals

$$
\bar{T} = \int_{-\frac{h}{2}}^{\frac{h}{2}} \alpha T\,dx_3 \ , \qquad M_T = \int_{-\frac{h}{2}}^{\frac{h}{2}} x_3 \alpha T\,dx_3
$$

The symbol D' used above is defined by $D' = \frac{Eh}{1-\nu^2}$. The subscript (,) represents the partial differentiation with respect to the following coordinates.

In case T is not a function of x_3

$$
\begin{aligned}
U_T &= -\frac{E}{1-\nu}\iint_S (\epsilon_x+\epsilon_\phi)\bar{T} B\,dx\,d\phi \\
&= -\frac{Eh}{1-\nu}\iint_S \Big[u_{,x} + \frac{1}{2}(w_{,x})^2 + \frac{1}{B}v_{,\phi} + \frac{u}{B}B_{,x} - k_\phi w + \\
&\qquad + \frac{1}{2}\left(\frac{1}{B}w_{,\phi}\right)^2 \Big] \alpha T B\,dx\,d\phi \qquad (2.13)
\end{aligned}
$$

The kinetic energy of the shell can be expressed as

$$
\begin{aligned}
V &= \frac{\rho}{2}\iint_S \left\{ \int_{-\frac{h}{2}}^{\frac{h}{2}} \left[(\dot{u} + x_3\dot{w}_{,x})^2 + \left(\dot{v} + x_3\frac{\dot{w}_{,\phi}}{B}\right)^2 + \dot{w}^2 \right] dx_3 \right\} \\
&\qquad B\,dx\,d\phi \\
&= \frac{\rho}{2}\iint_S \left\{ h(\dot{u}^2+\dot{v}^2+\dot{w}^2) + \frac{h^3}{12}(\dot{w}_{,x})^2 + \frac{h^3}{12}\left(\frac{\dot{w}_{,\phi}}{B}\right)^2 \right\} B\,dx\,d\phi \qquad (2.14)
\end{aligned}
$$

where the dot ($\dot{}$) represents $\frac{\partial}{\partial t}$, ρ is the mass density. Since the shell is assumed thin, the rotatory inertia terms can be reasonably neglected. Also for thin shallow shells, as Reissner [20] pointed out in his work that the tangential inertia forces can be ignored with negligible errors, the inertia effect considered in this dissertation is limited only to the inertia effect along the normal direction. Thus,

$$V = \frac{\rho h}{2} \iint_S (\dot{w})^2 B \, dx \, d\phi \tag{2.15}$$

For solving the present shell problems, the Hamilton principle is adopted. This principle states that among all the admissible states of stress the actual one is that which satisfies

$$\delta \int_{t_1}^{t_2} (V - U) \, dt = 0 \tag{2.16'}$$

where δ is a variational symbol, and U, V are the strain energy and the kinetic energy, respectively.

Expression (2.16') can be arranged to a more suitable form for applying the direct variational method. Since

$$\delta \int_{t_1}^{t_2} V \, dt = \delta \int_{t_1}^{t_2} \Big[\iint_S \frac{\rho h}{2} (\dot{w})^2 B \, dx \, d\phi \Big] dt$$

$$= \int_{t_1}^{t_2} \Big[\iint_S \rho h \, \dot{w} \, \delta \dot{w} \, B \, dx \, d\phi \Big] dt$$

One can integrate this expression by parts with respect to t, to yield

$$\delta \int_{t_1}^{t_2} V \, dt = \int_{t_1}^{t_2} \Big[\iint_S - \rho h (\ddot{w} \, \delta w) B \, dx \, d\phi \Big] dt +$$

$$+ \Big[\iint_S - \rho h (\dot{w} \, \delta w) B \, dx \, d\phi \Big]_{t_1}^{t_2}$$

The variation of the normal displacement, for the present problem, is always assumed zero at both terminals of the time interval. Therefore, it gives

$$\delta\int_{t_1}^{t_2} V\,dt = \int_{t_1}^{t_2}\Big[\iint_S -\rho h(\ddot{w}\,\delta w)\,B\,d\alpha\,d\phi\Big]\,dt$$

Thus, Equation (2.16') can be written in a new form

$$\int_{t_1}^{t_2}\Big[\iint_S \rho h(\ddot{w}\,\delta w)B\,d\alpha\,d\phi + \delta U\Big]\,dt \tag{2.16}$$

This expression is the actual one which will be used to carry out the direct variational calculations in the present dissertation.

2.4 Boundary Conditions and Initial Conditions

In this dissertation, the boundary conditions are simply supported and are completely restrained at both ends. These conditions can be formulated as

$$W = u = v = 0 \quad \text{at} \quad \begin{cases} x = x_1, x_2 & \text{(conical shell)} \\ x = \pm L/2 & \text{(cylindrical shell)} \end{cases}$$

$$M_x = -D(r_1^{-1} + \nu r_2^{-1}) = 0 \quad \text{at} \quad \begin{cases} x = x_1, x_2 & \text{(conical shell)} \\ x = \pm L/2 & \text{(cylindrical shell)} \end{cases} \tag{2.17}$$

where M_x is the longitudinal bending moment.

The initial conditions, for $t = 0$, are assumed to be

$$w = \dot{w} = 0 \tag{2.18}$$

2.5 Method of Approach

As it has been stated in the first chapter, the solution is carried out in two steps. The displacements, stresses and moments in the shell before buckling are found first. In the prebuckling state, the deformations are assumed symmetric. Thus, $v'=0$, and u' and w' depend on (x,t) only. The superscript ($'$) is applied to quantities at unbuckled state. The second step of the solution is to study the buckling relations for the linear case and the post-buckling relations for the nonlinear case. The superscript ($''$) is used to define the additional quantities due to buckling, or after buckling. The additional displacement components are denoted by (u'', v'', w''). They are the functions of (x, ϕ, t). Both (u', w') and (u'', v'', w'') are chosen to satisfy the boundary conditions.

It has been known that the shell deformations before buckling agree well with the classical theory of shells. This means that the quadratic terms of the strain components $\epsilon_x, \epsilon_\phi, \epsilon_{x\phi}$ have nothing but a negligible influence to the solution of prebuckling deformations, stresses and moments. Therefore, the strain components can be separated into two parts $\epsilon'_x, \epsilon''_x$; $\epsilon'_\phi, \epsilon''_\phi$ and $\epsilon'_{x\phi}, \epsilon''_{x\phi}$ of which all the strains with the superscript ($'$) are linear strains, and those with the superscript ($''$) are the additional nonlinear strains. They can be expressed as

$$\epsilon'_x = u_{,x} \tag{2.19a}$$

$$\epsilon'_\phi = \frac{1}{B} v_{,\phi} + \frac{u}{B} B_{,x} - R_\phi w \tag{2.19b}$$

$$\epsilon'_{x\phi} = \frac{1}{2}\left[v_{,x} + \frac{1}{B} u_{,\phi} - \frac{v}{B} B_{,x} \right] \tag{2.19c}$$

$$\epsilon''_x = \frac{1}{2} (w_{,x})^2 \tag{2.20a}$$

$$\epsilon''_\phi = \frac{1}{2} \left(\frac{1}{B} w_{,\phi} \right)^2 \tag{2.20b}$$

$$\epsilon''_{x\phi} = \frac{1}{B} w_{,x} w_{,\phi} \tag{2.20c}$$

For the prebuckling solution of deformations, stresses and moments, ϵ_x', ϵ_ϕ' and $\epsilon_{x\phi}'$ instead of ϵ_x, ϵ_ϕ, $\epsilon_{x\phi}$ are substituted in Equations (2.7), (2.10) and (2.13). Then, according to the conditions (2.17), the displacement functions u' and w' are assumed. The amplitudes of u' and w' are functions of time and known as generalized coordinates. Let u' and w' replace u and w, respectively, in the modified Equations (2.10), (2.13) and (2.11), (2.15). After integration over the total middle surface, the Hamilton principle is applied to establish the equations needed for solving the generalized coordinates of u' and w'. The thermal stresses (σ_x', σ_ϕ', $\sigma_{x\phi}'$) and the thermal moments (M_x', M_ϕ', $M_{x\phi}'$) are thus determined from the modified Equations (2.7) and (2.9), with $v \equiv 0$ and u, w replaced by u', w'.

During buckling, the slope changes of the shell deformation increase rapidly, and additional stresses (σ_x'', σ_ϕ'', $\sigma_{x\phi}''$) and additional moments (M_x'', M_ϕ'', $M_{x\phi}''$) are induced. At this stage, the classical theory of shells can no longer handle this problem. The additional strain energy developed from the influences of the nonlinear strain effect, and the additional stresses and moments must be introduced to justify the result of the present problem. Nevertheless, the direct coupling terms of the nonlinear strains and the additional stresses still remain to be small quantities of higher order, and can be neglected at this stage without serious error. Thus, one can formulate the membrane strain energy during buckling by the following steps. First, the additional stresses and nonlinear strains are added to the prebuckling stresses and linear strains to formulate the membrane strain energy as

$$\delta U_m = h\iint_S [(\sigma_x' + \sigma_x'')\,\delta(\epsilon_x' + \epsilon_x'') + (\sigma_\phi' + \sigma_\phi'')\,\delta(\epsilon_\phi' + \epsilon_\phi'') +$$

$$+ (\sigma_{x\phi}' + \sigma_{x\phi}'')\,\delta 2(\epsilon_{x\phi}' + \epsilon_{x\phi}'')]\, B\,dx\,d\phi$$

$$= h\iint_S (\sigma_x'\,\delta\epsilon_x' + \sigma_\phi'\,\delta\epsilon_\phi' + 2\sigma_{x\phi}'\,\delta\epsilon_{x\phi}')\,B\,dx\,d\phi +$$

$$+ h\iint_S (\sigma_x'\,\delta\epsilon_x'' + \sigma_\phi'\,\delta\epsilon_\phi'' + 2\sigma_{x\phi}'\,\delta\epsilon_{x\phi}'')\,B\,dx\,d\phi +$$

$$+ h\iint_S (\sigma_x''\,\delta\epsilon_x' + \sigma_\phi''\,\delta\epsilon_\phi' + 2\sigma_{x\phi}''\,\delta\epsilon_{x\phi}')\,B\,dx\,d\phi +$$

$$+ h\iint_S (\sigma_x''\,\delta\epsilon_x'' + \sigma_\phi''\,\delta\epsilon_\phi'' + 2\sigma_{x\phi}''\,\delta\epsilon_{x\phi}'')\,B\,dx\,d\phi \qquad (2.21)$$

Second, the last integral of Equation (2.21) is dropped according to the above argument, and (σ_x'', σ_ϕ'', $\sigma_{x\phi}''$) are expressed by the Equation (2.7) with ($\epsilon_x, \epsilon_\phi, \epsilon_{x\phi}$) replaced by (ϵ_x', ϵ_ϕ', $\epsilon_{x\phi}'$) and with the temperature terms missing. Thus,

$$\delta U_m = h\delta\iint_S (\sigma_x'\epsilon_x' + \sigma_\phi'\epsilon_\phi' + 2\sigma_{x\phi}'\epsilon_{x\phi}')\,B\,dx\,d\phi +$$

$$+ h\delta\iint_S (\sigma_x'\epsilon_x'' + \sigma_\phi'\epsilon_x'' + 2\sigma_{x\phi}'\epsilon_{x\phi}'')\,B\,dx\,d\phi +$$

$$+ \frac{D'}{2}\,\delta\iint_S [(\epsilon_x')^2 + (\epsilon_\phi')^2 + 2\nu\epsilon_x'\epsilon_\phi' + 2(1-\nu)(\epsilon_{x\phi}')^2]\,B\,dx\,d\phi$$

and finally,

$$U_m = h\iint_S (\sigma_x'\epsilon_x' + \sigma_\phi'\epsilon_\phi' + 2\sigma_{x\phi}'\epsilon_{x\phi}')\,B\,dx\,d\phi +$$

$$+ h\iint_S (\sigma_x'\epsilon_x'' + \sigma_\phi'\epsilon_\phi'' + 2\sigma_{x\phi}'\epsilon_{x\phi}'')\,B\,dx\,d\phi +$$

$$+ \frac{D'}{2}\iint_S [(\epsilon_x')^2 + (\epsilon_\phi')^2 + 2\nu\epsilon_x'\epsilon_\phi' + 2(1-\nu)(\epsilon_{x\phi}')^2]\,B\,dx\,d\phi \qquad (2.22)$$

As far as the bending strain energy is concerned, one can formulate it in the following straightforward form

$$\delta U_b = \iint_S \Big[(M_x' + M_x'')\,\delta(r_x^{-1}) + (M_\phi' + M_\phi'')\,\delta(r_\phi^{-1}) +$$

$$+ 2\,(M_{x\phi}' + M_{x\phi}'')\,\delta(r_{x\phi}^{-1}) \Big]\, B\, dx\, d\phi$$

in which ($M_x', M_\phi', M_{x\phi}'$) are the prebuckling moments. If the variational symbol δ is removed as it has been done in deriving the membrane strain energy expression during buckling, the bending strain energy will assume the following form

$$U_b = \iint_S \Big[M_x' r_x^{-1} + M_\phi' r_\phi^{-1} + 2 M_{x\phi}' r_{x\phi}^{-1} \Big]\, B\, dx\, d\phi \; +$$

$$+ \frac{D}{2} \iint_S \Big[(r_x^{-1})^2 + (r_\phi^{-1})^2 + 2\nu (r_x^{-1})(r_\phi^{-1}) + 2(1-\nu)(r_{x\phi}^{-1})^2 \Big]\, B\, dx\, d\phi \tag{2.23}$$

The displacement components u'', v'', w'' are assumed, and their amplitudes are again functions of time. Substituting the assumed u'', v'', w'' in Equations (2.8), (2.19), (2.20) and (2.15), then integrating Equations (2.15), (2.22), (2.23) over the total middle surface of the shell, the strain energy during buckling, $U = U_m + U_b$, and the kinetic energy during buckling, V , will be obtained. Applying the Hamilton principle to the new U and new V , a second order linear differential equation for the generalized coordinate of w'' with variable coefficient is obtained. This differential equation will be of the Mathieu type in this dissertation. So the dynamic stability of the shells calculated through a linear theory of the shallow thin shell will be discussed according to its properties shown in the Mathieu diagram.

After the buckling, the slope changes of the shell deformation become larger and larger; also, the additional stresses and moments tend to be larger and larger. In this case, large deformation theory (nonlinear theory) of shallow thin shells must be used to establish the strain energy expression. That is to say, the last term in Equation (2.21) should be retained to establish the membrane strain energy. Thus, if one expresses (σ_x'', σ_ϕ'', $\sigma_{x\phi}''$) by Equation (2.7) with the temperature terms missing, the membrane strain energy expression after the buckling will be obtained through the following procedure

$$
\begin{aligned}
\delta U_m = {} & h\,\delta \iint_S (\sigma_x' \epsilon_x' + \sigma_\phi' \epsilon_\phi' + 2\,\sigma_{x\phi}' \epsilon_{x\phi}')\, B\, dx\, d\phi\; + \\
& + h\,\delta \iint_S (\sigma_x' \epsilon_x'' + \sigma_\phi' \epsilon_\phi'' + 2\,\sigma_{x\phi}' \epsilon_{x\phi}'')\, B\, dx\, d\phi\; + \\
& + D' \iint_S [(\epsilon_x + \nu \epsilon_\phi)\,\delta \epsilon_x' + (\epsilon_\phi + \nu \epsilon_x)\,\delta \epsilon_\phi' + 2(1-\nu)\,\epsilon_{x\phi}\,\delta \epsilon_{x\phi}']\, B\, dx\, d\phi\; + \\
& + D' \iint_S [(\epsilon_x + \nu \epsilon_\phi)\,\delta \epsilon_x'' + (\epsilon_\phi + \nu \epsilon_x)\,\delta \epsilon_\phi'' + 2(1-\nu)\,\epsilon_{x\phi}\,\delta \epsilon_{x\phi}'']\, B\, dx\, d\phi \\
= {} & h\,\delta \iint_S (\sigma_x' \epsilon_x' + \sigma_\phi' \epsilon_\phi' + 2\sigma_{x\phi}' \epsilon_{x\phi}')\, B\, dx\, d\phi\; + \\
& + h\,\delta \iint_S (\sigma_x' \epsilon_x'' + \sigma_\phi' \epsilon_\phi'' + 2\,\sigma_{x\phi}' \epsilon_{x\phi}'')\, B\, dx\, d\phi\; + \\
& + \frac{D}{2}\,\delta \iint_S [\epsilon_x^2 + \epsilon_\phi^2 + 2\,\nu \epsilon_x \epsilon_\phi + 2(1-\nu)\,\epsilon_{x\phi}^2]\, B\, dx\, d\phi
\end{aligned}
$$

$$
\begin{aligned}
U_m = {} & h \iint_S (\sigma_x' \epsilon_x' + \sigma_\phi' \epsilon_\phi' + 2\sigma_{x\phi}' \epsilon_{x\phi}')\, B\, dx\, d\phi\; + \\
& + h \iint_S (\sigma_x' \epsilon_x'' + \sigma_\phi' \epsilon_\phi'' + 2\,\sigma_{x\phi}' \epsilon_{x\phi}'')\, B\, dx\, d\phi\; + \\
& + \frac{D'}{2} \iint_S [\epsilon_x^2 + \epsilon_\phi^2 + 2\,\nu \epsilon_x \epsilon_\phi + 2(1-\nu)\,\epsilon_{x\phi}^2]\, B\, dx\, d\phi
\end{aligned}
\tag{2.24}
$$

The bending strain energy expression will still remain Equation (2.23).

The displacement components u'', v'', w'' are again assumed, and their amplitudes are also functions of time. Substituting the assumed u'', v'', w'' in Equations (2.6), (2.8), (2.19) and (2.20), then integrating Equations (2.15), (2.23) and (2.24) over the total middle surface of the shell, the strain energy after buckling, $U = U_m + U_b$, and the kinetic energy after buckling, V, will be obtained. Applying the Hamilton principle to the new U and new V, a second order nonlinear differential equation for the generalized coordinate of w'' with variable coefficient is presented. This nonlinear differential equation will be used to study the dynamic stability of the shells.

CHAPTER 3

LINEAR SOLUTIONS

3.1 Conical Shells

In this section, Equations (2.2) and (2.4) are used to substitute the scale factor B and the curvature of the shell k_ϕ in all equations listed thereafter in Chapter 2. The procedure of solving these equations has been explained already in Section 2.5. Now, the detailed analysis of this portion will be given in the following sub-sections.

3.1.1 Transformation of coordinates

According to Mushtari and Sachenkov [32], the simply supported boundary conditions of conical shells can be satisfied by introducing

$$\xi = \log_e (x/x_1)$$

or

$$x = x_1 e^{\xi} \tag{3.1}$$

Thus, at the ends of the cones $x = x_1$ and x_2; correspondingly, $\xi = 0$ and ξ_0(i.e., $e^{\xi_0} = x_2/x_1$). For convenience, transformation is also made by defining

$$\Psi = \phi \sin\theta \tag{3.2}$$

According to Equations (3.1) and (3.2), the following relations hold

$$\frac{\partial}{\partial x} = (x_1 e^{\zeta})^{-1}\left(\frac{\partial}{\partial \zeta}\right)$$

$$\frac{\partial^2}{\partial x^2} = (x_1 e^{\zeta})^{-2}\left(\frac{\partial^2}{\partial \zeta^2} - \frac{\partial}{\partial \zeta}\right)$$

$$(x \,\mathrm{Sin}\theta)^{-1}\left(\frac{\partial}{\partial \phi}\right) = (x_1 e^{\zeta})^{-1}\left(\frac{\partial}{\partial \psi}\right) \tag{3.3}$$

$$(x \,\mathrm{Sin}\theta)^{-2}\left(\frac{\partial^2}{\partial \phi^2}\right) = (x_1 e^{\zeta})^{-2}\left(\frac{\partial^2}{\partial \psi^2}\right)$$

$$\frac{\partial}{\partial x}\left[(x \,\mathrm{Sin}\theta)^{-1}\frac{\partial}{\partial \phi}\right] \quad (x_1 e^{\zeta})^{-2}\left(\frac{\partial^2}{\partial \zeta \partial \psi} - \frac{\partial}{\partial \psi}\right)$$

By using this transformation, all the basic expressions in the preceding chapter are transformed depending upon coordinates ζ and ψ .

3.1.2 The prebuckling solution

If one assumes the temperature load $T = T(t)$, i.e., the temperature is applied uniformly over the shell surface, and there is no temperature gradient through the thickness of the shell, then one can reasonably expect that the deformation before buckling is symmetric. In this case, as it has been stated in the preceding chapter, all the terms concerning v and $\frac{\partial}{\partial \psi}$ vanish. The displacements prior to buckling are assumed as

$$u' = Q_u'(t)\,\mathrm{Sin}\left(\frac{2\pi\zeta}{\zeta_0}\right) + \left[(1+\nu)\alpha T \zeta_0 x_1 e^{\zeta}/2\pi\right]\mathrm{Sin}\left(\frac{2\pi\zeta}{\zeta_0}\right) \tag{3.4a}$$

$$w' = Q_w'(t)\, e^{\lambda\zeta}\,\mathrm{Sin}\left(\frac{\pi\zeta}{\zeta_0}\right) \tag{3.4b}$$

in which $\zeta_0 = \log_e(x_2/x_1)$, $\lambda = \frac{1-\nu}{2}$, $Q_u'(t)$ and $Q_w'(t)$ are the amplitudes of u' and w' . The additional term $\left[(1+\nu)\alpha T \zeta_0 x_1 e^{\zeta}/2\pi\right]\mathrm{Sin}\left(\frac{2\pi\zeta}{\zeta_0}\right)$

is introduced for the purpose of satisfying the equilibrium condition

$$[2\pi x_1 h \tan\theta\, \sigma_x]_{x=x_1} = [2\pi x_2 h \tan\theta\, \sigma_x]_{x=x_2}$$

The method to establish the strain energy and kinetic energy has already been given in Section (2.5). The integration of these energy expressions are carried out over the limits ($\zeta = 0$ to $\zeta = \zeta_0$, $\psi = 0$ to $\psi = 2\pi \sin\theta$). The Hamilton principle is applied by partially differentiating the integrand with respect to the generalized coordinates Q_u' and Q_w' and setting the results to equal zero separately. Thus, it gives one algebraic equation which relates Q_u' and Q_w' by

$$Q_u' = F_1 Q_w' + F_3 \alpha T \tag{3.5}$$

and another differential equation of Q_w' with Q_u' coupled in it. Considering Equation (3.5) in this differential equation, the function Q_w' is determined by

$$\frac{\rho R_1^2 (1-\nu^2)}{E} \frac{d^2 Q_w'}{dt^2} + \omega^2 Q_w' = F_2 \alpha T \tag{3.6}$$

where F_1 is a function of (ν, ζ_0, θ) and F_2, F_3 depend on the parameters ($\nu, R_1, \zeta_0, \theta$). ω^2 is a function of ($\nu, R_1, \zeta_0, \theta, h$). All F_1, F_2, F_3, ω^2 are expressed in terms of ($\nu, h, R_1, \theta, \zeta_0$) in Appendix I. Physically, ω assumes the natural frequency and ($F_2 \alpha T$) behaves as a thermal-force. The initial conditions of Q_w' are reduced from Equation (2.18) as

$$Q_w' = \dot{Q}_w' = 0 \qquad \text{at} \qquad t = 0$$

The solution of Q_w' will depend on the temperature function T .

The first type of temperature function under study is sinusoidal. It assumes

$$T = T_0 \cos(\omega_1 t) \tag{3.7}$$

where T_0 is a constant and ω_1 is the frequency of the temperature loading. The solution of Equation (3.6) is so obvious that it can be obtained by simply applying the Laplace transform. It is written as

$$(Q_w')_S = \frac{F_2 \alpha T_0}{\omega^2 - \Omega_1^2} \cos(\Omega_1 \tau) \tag{3.8}$$

where $\Omega_1 \tau = \omega_1 t$ and $\tau = \left[\frac{E}{\rho R_1^2 (1-\nu^2)}\right]^{\frac{1}{2}} t$. The subscript S is introduced for the case of sinusoidal temperature function. Using Equations (3.8) and (3.5) in Equation (3.4), the prebuckling displacements due to sinusoidal temperature gradient are then determined.

The second temperature function is chosen as

$$\begin{aligned} T &= T_1 t / t_0 \quad &\text{for} \quad & 0 < t < t_0 \\ T &= T_1 \quad &\text{for} \quad & t \geq t_0 \end{aligned} \tag{3.9}$$

where T_1 is a constant.

In accordance with the conditions given in Equations (2.18) and (3.9), the solution of Q_w' from Equation (3.6) can be obtained as follows. Let

$$\bar{t} = \frac{t}{\tau} = \left[\frac{E}{\rho R_1^2 (1-\nu^2)}\right]^{-\frac{1}{2}}$$

Applying the Laplace transform to Equation (3.6) yields

$$Q_w' = \frac{\alpha T_1 \bar{t} F_2}{\omega^3 t_0} \left[\omega\tau - \sin(\omega\tau)\right]$$

$$\frac{dQ_w'}{d\tau} = \frac{\alpha T_1 \bar{t} F_2}{\omega^2 t_0} \left[1 - \cos(\omega\tau)\right]$$

at $t = t_0$ or $\tau = \frac{t_0}{\bar{t}}$.

$$Q'_w = \frac{\alpha T_1 F_2}{\omega^3}\left[\omega - \frac{\bar{t}}{t_0}\sin\left(\frac{\omega t_0}{\bar{t}}\right)\right] \qquad (3.10a)$$

$$\frac{dQ'_w}{d\tau} = \frac{\alpha T_1 \bar{t} F_2}{\omega^2 t_0}\left[1 - \cos\left(\frac{\omega t_0}{\bar{t}}\right)\right] \qquad (3.10b)$$

When $t > t_0$, taking $t = t_0$ as the initial stage by considering Equation (3.10) as the initial condition, the solution of $(Q'_w)_r$ is obtained by superimposing the particular solution, which again can be obtained through the Laplace transform and the complementary solution of Equation (3.6), where the subscript r refers the quantities to the case of ramp-type thermal loading. The explicit expression of $(Q'_w)_r$ can be written as

$$(Q'_w)_r = \frac{F_2 \alpha T_1}{\omega^2}\left[1 - \frac{1}{\omega}\frac{\bar{t}}{t_0}\left(2 - 2\cos\left(\frac{\omega t_0}{\bar{\tau}}\right)\right)^{\frac{1}{2}}\cos\bar{\tau}\right] \qquad (3.11)$$

In Equation (3.11)

$$\bar{\tau} = \omega(\tau - \tau_0/\bar{\tau}) + A_4$$

where A_4 is a phase angle.

For a Heavyside load, $t_0 = 0$ and

$$(Q'_w)_h = \frac{\alpha T_1 F_2}{\omega^2}(1 - \cos\bar{\tau}) \qquad (3.12)$$

where the subscript h refers the quantity to the case of a Heavyside load.

Using Equations (3.5) and (3.11) or (3.12) in Equation (3.4), the prebuckling displacements due to a ramp-type temperature loading or a Heavyside temperature loading are thus determined.

The thermal stresses and moments are obtained by using the above solutions to the prebuckling displacements in Equation (2.7). Of course, the quadratic terms related to the normal displacement, and other terms related to v and $\frac{\partial}{\partial \phi}$ in Equation (2.7) are dropped in this case.

3.1.3 Considerations of dynamic stability during buckling

During buckling, the additional displacement components are chosen in the following forms

$$u''= Q''_u(t)\,\mathrm{Sin}\left(\frac{2m\pi z}{z_0}\right)\mathrm{Cos}\,(n_1\psi) \tag{3.13a}$$

$$v''= Q''_v(t)\,\mathrm{Sin}\left(\frac{m\pi z}{z_0}\right)\mathrm{Sin}\,(n_1\psi)\,e^{\lambda z} \tag{3.13b}$$

$$w''= Q''_w(t)\,\mathrm{Sin}\left(\frac{m\pi z}{z_0}\right)\mathrm{Cos}\,(n_1\psi)\,e^{\lambda z} \tag{3.13c}$$

where m is an odd integer and $n_1 = n/\mathrm{Sin}\,\theta$, in which n is an integer. The Lagrangian function used in the Hamilton principle is, as it has been stated in Section 2.5, the sum of Equations (2.15) (with negative sign), (2.22) and (2.23). The direct variational operation to Equation (2.16) gives three coupled equations of the generalized coordinates Q''_u, Q''_v and Q''_w. Two of them are algebraic equations and can be arranged to express Q''_u, Q''_v in terms of Q''_w. The third one is a differential equation with variable coefficient. By considering the first two equations, this differential equation can be arranged to become a Mathieu type with only Q''_w as its argument.

For sinusoidal temperature load, they are

$$(Q''_u)_s = F_4\,(Q''_w)_s \tag{3.14a}$$

$$(Q''_v)_s = F_5\,(Q''_w)_s \tag{3.14b}$$

$$\frac{d^2(Q''_w)_s}{d\bar{\bar{\tau}}^2} + \frac{\Omega^2_{mn}}{\Omega^2_1}\left(1 - \frac{T_0}{T_{cr}}\cos\bar{\bar{\tau}}\right)(Q''_w)_s = 0 \tag{3.14c}$$

where

$$\bar{\bar{\tau}} = \Omega_1 \tau$$

$$\Omega_{mn} = \text{frequency parameter}$$

In general, F_4 and F_5 are functions of (ζ_0, θ, m, n), the frequency function Ω^2_{mn} depends on ($\zeta_0, \theta, R_1/h, m, n$) and the function T_{cr} is a function of ($\zeta_0, \theta, R_1/h, m, n, \alpha$). When $\Omega_1 = 0$, i.e., $\omega_1 = 0$, the smallest value of T_{cr} with respect to m, n assumes the static-buckling temperature and is denoted by $(T_{cr})_{st}$.

For ramp-type thermal loading, the final equations take the following forms

$$(Q''_u)_r = F_4 \, (Q''_w)_r \tag{3.15a}$$

$$(Q''_v)_r = F_5 \, (Q''_w)_r \tag{3.15b}$$

$$\frac{d^2 (Q''_w)_r}{d\bar{\tau}^2} + \frac{\Omega^2_{mn}}{\omega^2}\left(1 - \frac{T_1}{T_{cr}} - \frac{T_1}{T_r}\cos\bar{\tau}\right)(Q''_w)_r = 0 \tag{3.15c}$$

where T_r is a function of ($\zeta_0, \theta, R_1/h, m, n, \alpha$). All F_4, F_5, Ω^2_{mn}, T_{cr} and T_r are expressed in Appendix I. The region of stability is determined from the parameters in Equations (3.14c) or (3.15c).

3.2 Cylindrical Shells

In this section, Equations (2.3) and (2.5) are used to substitute the scale factor B and the curvature of the shell k_ϕ in all equations listed thereafter in Chapter 2. The procedure of obtaining the final equations which indicate the characteristics of dynamic stability of this kind of shell is parallel to that stated in Section 3.1.

Therefore, in the following sub-sections, results will be simply given without further explanation.

3.2.1 The prebuckling solution

For a cylindrical shell, the displacement components prior to buckling are assumed as

$$u_c' = Q_{uc}'(t)\left(\sin\left(\frac{\pi x}{L}\right) - \frac{2x}{L}\right) \tag{3.16a}$$

$$w_c' = Q_{wc}'(t)\cos\left(\frac{\pi x}{L}\right) \tag{3.16b}$$

where the subscript c is used to indicate the case of cylindrical shells.

The integrations of energy expressions are carried out over the limit ($x = \pm L/2$, $\phi = 0$ to $\phi = 2\pi$). After the Hamilton principle is applied in a direct sense, the time-dependent amplitudes of u_c' and w_c' under a sinusoidal temperature loading are

$$(Q_{uc}')_s = \frac{\nu L}{\pi R}(Q_{wc}')_s \tag{3.17a}$$

$$(Q_{wc}')_s = F_7 \alpha T_0 \cos(\Omega_1 \tau)/(\omega_c^2 - \Omega_1^2) \tag{3.17b}$$

while under a ramp-type temperature load are

$$(Q_{uc}')_r = \frac{\nu L}{\pi R}(Q_{wc}')_r \tag{3.18a}$$

$$(Q_{wc}')_r = \frac{F_7}{\omega_c^2}\alpha T_1\left[1 - \frac{\bar{t}}{\omega_c t_0}\left(2 - 2\cos\left(\frac{\omega_c t_0}{\bar{t}}\right)^{\frac{1}{2}}\right]\cos(\omega_c \bar{\tau}) \tag{3.18b}$$

ω_c assumes the prior buckling natural frequency function. Both ω_c and F_7 are functions of (R, h, L, ν), and are expressed in Appendix II.

For a Heavyside load, $t_0 = 0$ and

$$(Q'_{uc})_h = \frac{\nu L}{\pi R}(Q'_{wc})_h \tag{3.19a}$$

$$(Q'_{wc})_h = \frac{\alpha T_1 F_1}{\omega_c^2}(1 - \cos\bar{\tau}) \tag{3.19b}$$

The thermal stresses and moments can be found in exactly the same way as in Section 3.1.2.

3.2.2 Considerations of dynamic stability during buckling

During buckling, the additional displacements are chosen in the following forms

$$u''_c = Q''_{uc}(t)\left[\sin\left(\frac{m\pi x}{L}\right) - (-1)^{\frac{m-1}{2}}\left(\frac{2x}{L}\right)\right]\sin(n\phi) \tag{3.20a}$$

$$v''_c = Q''_{vc}(t)\cos\left(\frac{m\pi x}{L}\right)\cos(n\phi) \tag{3.20b}$$

$$w''_c = Q''_{wc}(t)\cos\left(\frac{m\pi x}{L}\right)\sin(n\phi) \tag{3.20c}$$

where m is an odd integer, and n is an integer. After applying the Hamilton principle in a direct sense, the final governing relationship also assumes the type of Mathieu's differential equation. For a sinusoidal temperature load

$$\frac{d^2(Q''_{wc})_s}{d\bar{\bar{\tau}}^2} + \frac{(\Omega^c_{mn})^2}{\Omega_1^2}\left(1 - \frac{T_0}{T^c_{cr}}\cos\bar{\bar{\tau}}\right)(Q''_{wc})_s = 0 \tag{3.21}$$

For a ramp-type temperature load

$$\frac{d^2(Q''_{wc})_r}{d\bar{\tau}^2} + \frac{(\Omega^c_{mn})^2}{\Omega_1^2}\left(1 - \frac{T_1}{T^c_{cr}} - \frac{T_1}{T^c_r}\cos\bar{\tau}\right)(Q''_{wc})_r = 0 \tag{3.22}$$

where the superscript c is used to indicate the case of a cylindrical shell. In the above equations, $\bar{\tau} = \omega_c(\tau - \frac{t_0}{\bar{t}}) + \bar{\bar{A}}_4$, $\bar{\bar{A}}_4$ is the phase angle, Ω^c_{mn} is a function of $(L, \frac{R}{h}, m, n)$ and T^c_{cr} is a function of

$(\frac{R}{h}, L, \alpha, m, n)$. When ω_c equals zero, the smallest value of T_{cr}^c with respect to m, n represents the static-buckling temperature of the shell. The function T_r^c also depends upon $(\frac{R}{h}, L, \alpha, m, n)$. All $(\Omega_{mn}^c)^2$, T_{cr}^c, T_r^c are expressed in Appendix II. The region of stability is determined from the parameters in Equations (3.21) or (3.22).

3.3 Numerical Results and Discussions

The condition of dynamic stability depends upon the numerical values of the parameters in Equations (3.14c) or (3.15c) for conical shells and in Equations (3.21) or (3.22) for cylindrical shells. The geometric parameters used for the case of conical shells are $(\frac{\bar{R}}{h}, \frac{\bar{R}}{H}, \theta)$ where

$$\bar{R} = (R_1 + R_2)/2 \tag{3.23}$$

$$H = (x_2 - x_1)\cos\theta \tag{3.24}$$

The geometric parameters used for the cylindrical shells are R/h and R/L, where R and L are the radius and length, respectively. In the numerical calculation, Poisson's ratio, ν, is taken as 0.3. The length of ramp-type loading, t_o, is assumed to be $\pi\bar{t}$. For Heavyside loading, t_o is zero.

$\frac{\bar{R}}{h}$ = 200, 500, 1,000; $\frac{\bar{R}}{H}$ = 0.5, 1.0; θ = 3°, 10°, 20°;

$\frac{R}{h}$ = 200, 500, 1,000; $\frac{R}{L}$ = 0.2, 0.5, 1.0

Values of Ω_1 are given as shown in the figures.

The calculations are made by using IBM 709. A flow-diagram of the Fortran programme is given in Appendix III. The parameters are plotted in the diagrams of Mathieu's equation. In Figures 2 - 6, the shaded areas represent the stable region. These effects of the temperature frequency and geometry of the shell on the stability are discussed below.

3.3.1 Influence of the force frequency

From Figures 2 and 3, one can notice that the shells are more unstable when the force frequencies Ω_1 are close to the prior buckling natural frequencies ω_c and ω . This conclusion is similar to the conclusion of Bieniek, Fan and Lackman [11]. In reference [11], a cylindrical shell is considered under a harmonic external pressure. Shells with Ω_1 far away from and smaller than ω_c and ω have not any combination of m and n falling into the first unstable region. This can be interpreted that, for the low force frequency, the stability of a dynamic problem is approximately the same as the stability of a corresponding static problem of conical and cylindrical shells. Shells with Ω_1 far away from and greater than ω_c and ω will have some combinations of m and n falling into the first unstable region. This means that, for the high force frequency, the stability of a dynamic problem is quite different from that of a corresponding static problem of conical and cylindrical shells. In fact, it tells that for this case the stability of a dynamic problem is much more serious than the static one. The dangerous phenomenon of Ω_1 close to ω_c and ω can be explained by looking into Equations (3.8) and (3.17b). For a limiting case, say, $\Omega_1 = \omega_c$ or ω , then $(Q_w')_s$ and $(Q_{wc}')_s$ approach to infinity. This is the case of resonance of a force vibration. Theoretically speaking, the shells under these conditions can never be stable no matter how small the applied load is. Therefore, one can expect that force frequencies, closer to the resonance force frequency, provide more unfavorable conditions to the stability of the shell.

3.3.2 Influence of the radius-length parameter

According to Figures 4 and 5, the radius-length parameters $\frac{R}{L}$ and $\frac{\bar{R}}{H}$ are not important factors in dynamic stability problems of cylindrical and conical shells. This means that for a certain value of radius, thickness and apex angle (for conical shells), shells with different lengths will become unstable at approximately the same value of temperature under a harmonic thermal load. This statement is more exact for a cylindrical shell rather than a conical shell, because as one can see from the figures, the effect of length to conical shells is larger than the same effect to cylindrical shells. However, it seems that there is a certain characteristic difference between conical and cylindrical shells, since Figure 5 shows that the shorter the shell is, the easier it becomes unstable, while Figure 4 shows just the opposite. This difference is physically interpreted by considering the effect of the radius R_1 at the upper end of a conical shell. For the same $\bar{R}$, a longer shell has a smaller R_1. This makes it easier to become unstable. To verify this intuitive argument, Figure 6 is plotted under the parameter $\frac{R_1}{H}$. For the same R_1, Figure 6 shows that the shorter shell becomes unstable first. This agrees with the trend of the cylindrical shell. For the ramp-type temperature load, the effect of the radius-length parameter is also very small.

3.3.3 Influence of the radius-thickness parameter

From Figures 4, 5 and 6, one can immediately observe that the radius-thickness parameters $\frac{R}{h}$ and $\frac{\bar{R}}{h}$ are the most important geometric factors for dynamic stability problems of conical and cylindrical shells. These figures show that for the same value of the radius-length parameter and the apex angle (for conical shells), different values of

$\frac{R}{h}$ or $\frac{\bar{R}}{h}$ will influence the stability of the shell to different extents. The larger the value of $\frac{R}{h}$ or $\frac{\bar{R}}{h}$ is, or say, the thinner the shell is, the more unfavorable the condition of dynamic stability of the shell will be. This conclusion is in accordance with the conclusion of the static case. For a ramp-type temperature load or Heavyside temperature load, the conclusion is also the same as above. A series of curves are plotted in Figures 7 and 8.

3.3.4 Influence of the apex angle

In Figure 4, for each set of values of $\frac{\bar{R}}{H}$ and $\frac{\bar{R}}{h}$, three different values of the half-apex angle θ are imposed. The curves show that the apex angle, just as the length, plays an unimportant role in a dynamic stability problem of a conical shell. However, it reveals that the shell under a harmonic temperature load will be more unstable as the apex angle is increased. For a ramp-type temperature load, the conclusion is again the same as above.

3.3.5 Comparison between the effect of a ramp-type temperature load and a Heavyside temperature load

As it has been mentioned before, the Heavyside temperature load can be deduced from the ramp-type load simply by setting $t_0 = 0$. Therefore, in Figures 7 and 8, curves with $t_0 = 0$ and $t_0 = \pi \bar{t}$ are plotted separately with T_1 equal to the static-buckling temperature of the shell under uniform temperature load. The results show that the Heavyside temperature load is more unfavorable than the ramp-type temperature load. These results are also similar to the results of a cylindrical shell under the same types of external pressure [11]. In fact, these results can be expected intuitively. Since, if one transforms the origin of the time coordinate from $t = 0$ to $t = t_0$ for the ramp-type load, one will find that shells under a ramp-type load are actually the same as shells under a Heavyside load with initial deflection and velocity.

TABLE I

CONVERSION OF COEFFICIENTS OF THE LINEAR MATHIEU DIFFERENTIAL EQUATION

		γ	ζ
Conical Shell	Sinusoidal Temperature Loading	$\left(\frac{\Omega_{mn}}{\Omega_1}\right)^2$	$\left(\frac{\Omega_{mn}}{\Omega_1}\right)^2 \frac{T_0}{T_{cr}}$
	Ramp-type Temperature Loading	$\left(\frac{\Omega_{mn}}{\omega}\right)^2 \left(1 - \frac{T_1}{T_{cr}}\right)$	$\left(\frac{\Omega_{mn}}{\omega}\right)^2 \frac{T_1}{T_r}$
Cylindrical Shell	Sinusoidal Temperature Loading	$\left(\frac{\Omega^c_{mn}}{\Omega_1}\right)^2$	$\left(\frac{\Omega^c_{mn}}{\Omega_1}\right)^2 \frac{T_0}{T^c_{cr}}$
	Ramp-type Temperature Loading	$\left(\frac{\Omega^c_{mn}}{\omega_c}\right)^2 \left(1 - \frac{T_1}{T^c_{cr}}\right)$	$\left(\frac{\Omega^c_{mn}}{\omega_c}\right)^2 \frac{T_1}{T^c_r}$

The linear Mathieu differential equation: $\frac{d^2Q}{dy^2} + (\gamma - \zeta \cos y)Q = 0$, where Q in Equations (3.14c), (3.15c), (3.21) or (3.22) is Q''_w or Q''_{wc} and y in Equations (3.14c), (3.15c), (3.21) or (3.22) is $\bar{\bar{\tau}}$ or $\bar{\tau}$.

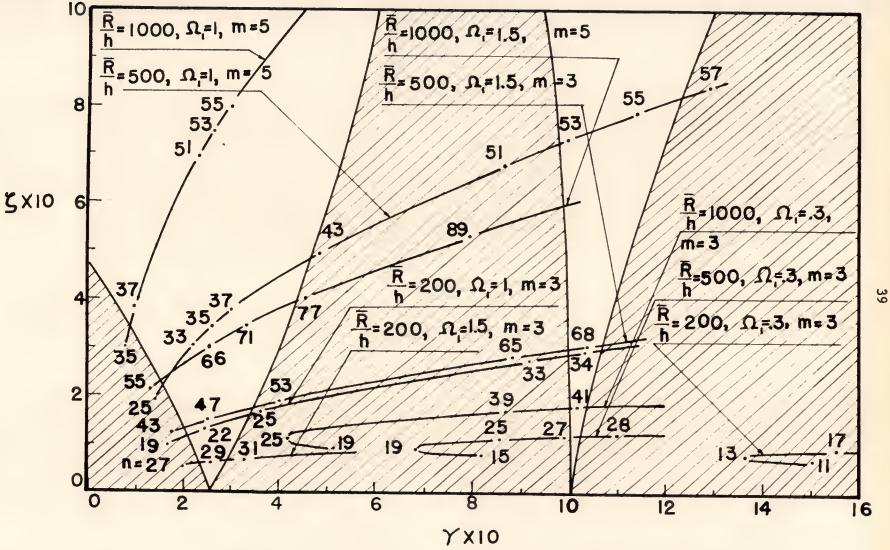

Figure 2. Mathieu's Diagram of Conical Shell under Sinusoidal Temperature Loading with Three Frequencies $\Omega_1 = 0.3$, 1.0, 1.5 ($\bar{R}/H = 1$, $\alpha T_0 = 3.5 \times 10^{-4}$, $\omega = 0.77$, $\theta = 20°$).

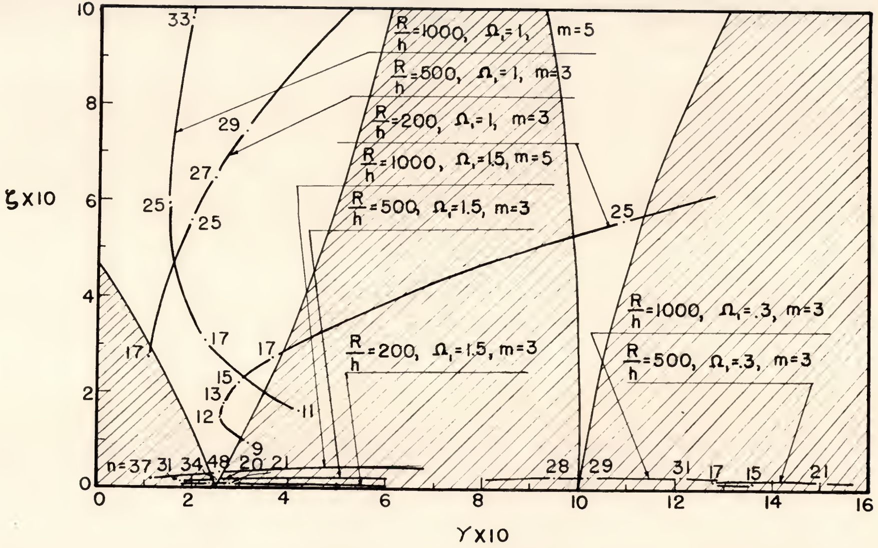

Figure 3. Mathieu's Diagram of Cylindrical Shell under Sinusoidal Temperature Loading with Three Frequencies $\Omega_1 = 0.3$, 1.0, 1.5, $(R/L = 1, \alpha T_0 = 0.13 \times 10^{-4}, \omega_c = 0.99)$.

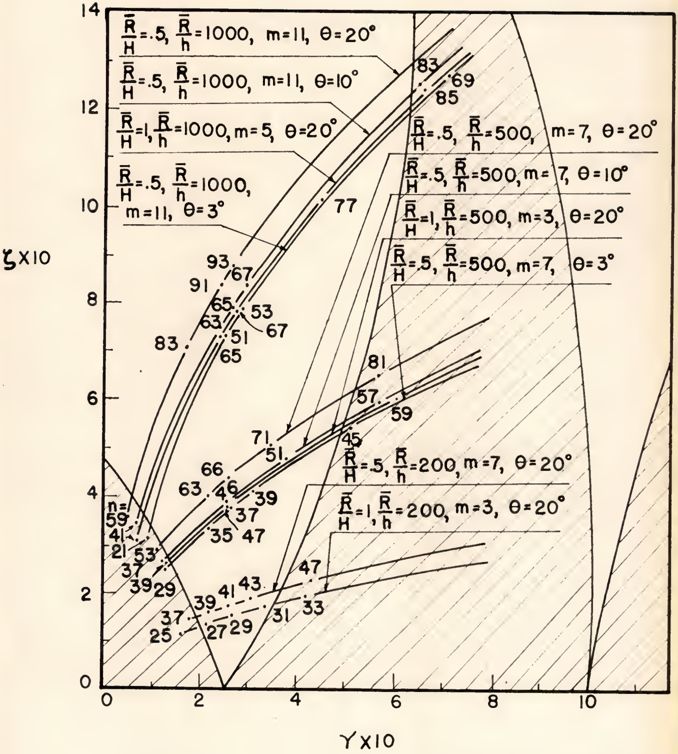

Figure 4. Mathieu's Diagram of a Conical Shell under Sinusoidal Temperature Loading ($\Omega_1 = 1.5$, $\alpha T_0 = 3.5 \times 10^{-4}$).

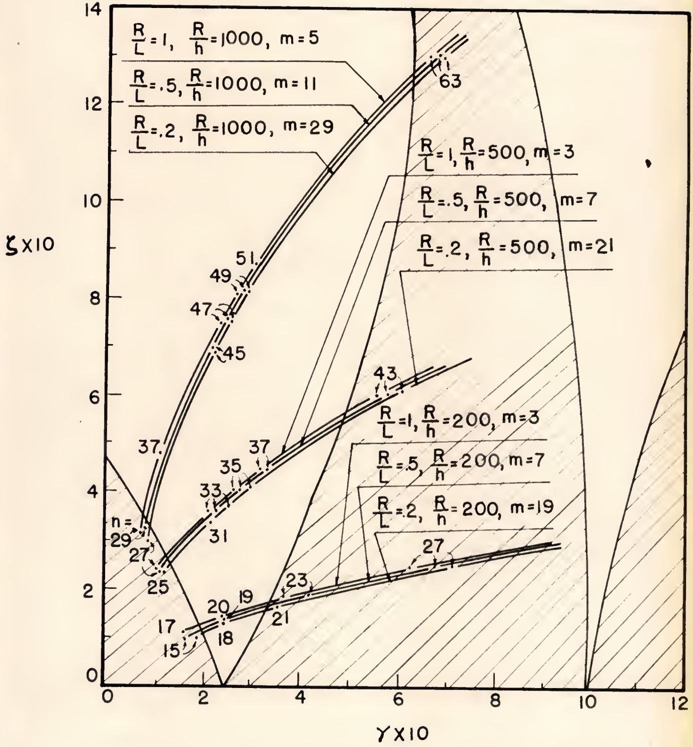

Figure 5. Mathieu's Diagram of a Cylindrical Shell under Sinusoidal Temperature Loading ($\Omega_1 = 1.5$, $\alpha T_0 = 3.5 \times 10^{-4}$).

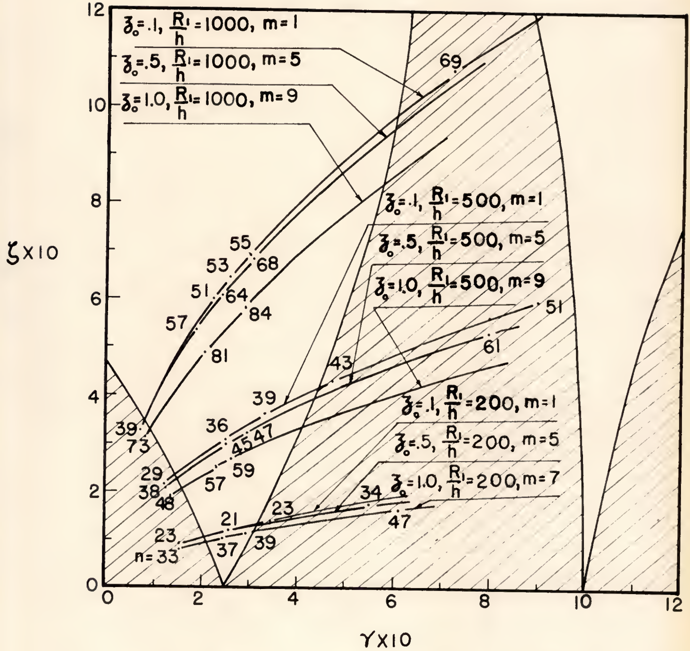

Figure 6. Mathieu's Diagram of a Conical Shell under Sinusoidal Temperature Loading ($\Omega_1 = 1.5$, $\alpha T_o = 3.5 \times 10^{-4}$, $\theta = 20°$).

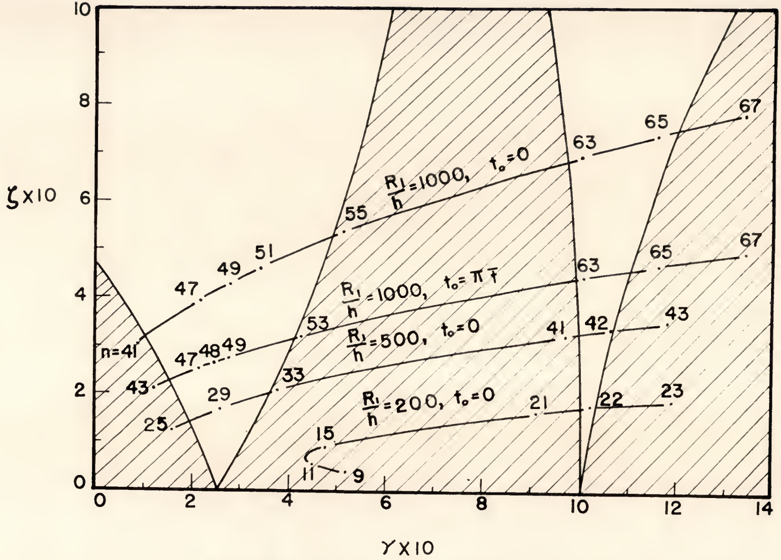

Figure 7. Mathieu's Diagram of a Conical Shell under Ramp-Type and Heavyside Temperature Loadings ($\zeta_0 = 0.1$, $\theta = 20°$, $T_1/(T_{cr})_{st} = 1$).

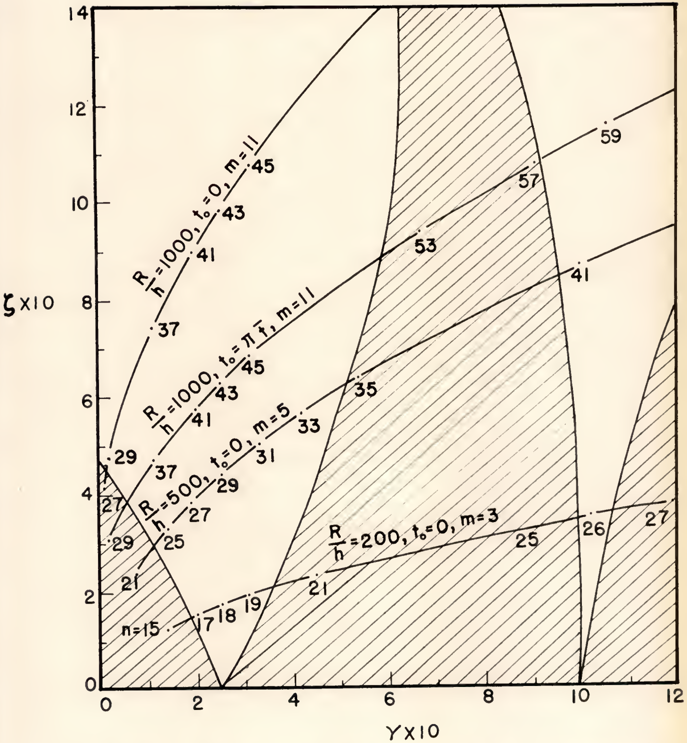

Figure 8. Mathieu's Diagram of a Cylindrical Shell under Ramp-Type and Heavyside Temperature Loadings ($L = 2R$, $T_1/(T^c_{cr})_{st} = 1$).

CHAPTER 4

NONLINEAR SOLUTIONS

4.1 Conical Shells

In this section, just as in Section 3.1, the scale factor B and the curvature of the shell k_ϕ, appearing in all basic equations of Chapter 2, are expressed by Equations (2.2) and (2.4). The coordinates (x, ϕ) are transformed to the pair of coordinates (z, ψ) through the transformation explained in Section 3.1.1. The detailed analysis of the conical shell through the procedure stated in Section 2.5 is given in the following sections.

4.1.1 Basic governing nonlinear differential equations

The prebuckling solution to the present case is exactly the same as obtained in Section 3.1.2. The prebuckling deformation is assumed to be symmetric. After buckling, the additional displacement components are chosen in the following forms

$$\mathcal{U}'' = A_1(t)\sin\left(\frac{2m\pi z}{z_0}\right)\cos(n_1\psi) + A_2(t)\sin\left(\frac{2m\pi z}{z_0}\right)\cos(2n_1\psi) + $$

$$+ A_3(t)\sin\left(\frac{2m\pi z}{z_0}\right) \tag{4.1a}$$

$$V'' = B_1(t)e^{\lambda z}\sin\left(\frac{\pi m z}{z_0}\right)\sin(n_1\psi) + $$

$$+ B_2(t)e^{\lambda z}\sin(2n_1\psi)\left[\cos\left(\frac{2m\pi z}{z_0}\right) - 1\right] \tag{4.1b}$$

$$W'' = C_1(t)e^{\lambda z}\sin\left(\frac{m\pi z}{z_0}\right)\cos(n_1\psi) \tag{4.1c}$$

where $A_1(t), A_2(t), A_3(t)$; $B_1(t), B_2(t)$ and $C_1(t)$ are time-dependent amplitudes of u'', v'' and w''. The additional terms $A_2(t)\,\mathrm{Sin}\left(\frac{2m\pi\zeta}{\zeta_0}\right)\mathrm{Cos}(2n_1\psi)$, $A_3(t)\,\mathrm{Sin}\left(\frac{2m\pi\zeta}{\zeta_0}\right)$ and $B_2(t)e^{\lambda\zeta}\left[\mathrm{Cos}\left(\frac{2m\pi\zeta}{\zeta_0}\right)-1\right]\mathrm{Sin}(2n_1\psi)$ are introduced for the purpose of showing the effects of the nonlinear coupling terms in the strain energy expression. If Equation (2.24) is expressed in terms of the displacement components u'', v'' and w'', it will assume the following form for the conical shell.

$$
\begin{aligned}
U_m = {} & h\int_0^{\zeta_0}\int_0^{2\pi\,\mathrm{Sin}\,\theta} \Big\{ \sigma_x' u''_{,\zeta} + \sigma_\phi'(v''_{,\psi} - \cot\theta\, w'' + u'') + \\
& + \sigma_{x\phi}'(v''_{,\zeta} + u''_{,\psi} - v'')\Big](x_1 e^{\zeta})\,d\zeta\, d\psi \; + \\
& + \frac{h}{2}\int_0^{\zeta_0}\int_0^{2\pi\,\mathrm{Sin}\,\theta} \left[\sigma_x'(w''_{,\zeta})^2 + \sigma_\phi'(w''_{,\psi})^2 + 2\sigma_{x\phi}'(w''_{,\zeta})(w''_{,\psi})\right] d\zeta\, d\psi \; + \\
& + \frac{D'}{2}\int_0^{\zeta_0}\int_0^{2\pi\,\mathrm{Sin}\,\theta} \Big[(u''_{,\zeta})^2 + (v''_{,\psi} - \cot\theta\, w'' + u'')^2 + 2\nu u''_{,\zeta}(v''_{,\psi} - \cot\theta\, w'' + \\
& + u'') + \frac{1-\nu}{2}(v''_{,\zeta} + u''_{,\psi} - v'')^2\Big] d\zeta\, d\psi \; + \\
& + \frac{D'}{2}\int_0^{\zeta_0}\int_0^{2\pi\,\mathrm{Sin}\,\theta} \left[(w''_{,\zeta})^4 + (w''_{,\psi})^4 + 2(w''_{,\zeta})^2(w''_{,\psi})^2\right](2x_1 e^{\zeta})^{-2} d\zeta\, d\psi \; + \\
& + \frac{D'}{2}\int_0^{\zeta_0}\int_0^{2\pi\,\mathrm{Sin}\,\theta} \Big[u''_{,\zeta}(w''_{,\zeta})^2 + (v''_{,\psi} - \cot\theta\, w'' + u'')(w_{,\psi})^2 + \nu u''_{,\zeta}(w''_{,\psi})^2 + \\
& + \nu(v''_{,\psi} - \cot\theta\, w'' + u'')(w''_{,\zeta})^2 + (1-\nu)(v''_{,\zeta} + u''_{,\psi} - v'')w''_{,\zeta} w''_{,\psi}\Big] \\
& (x_1 e^{\zeta})^{-1} d\zeta\, d\psi
\end{aligned}
\tag{4.2}
$$

If the additional terms are dropped from Equations (4.1a) and (4.1b), one can immediately observe that after Equations (4.1a), (4.1b) and (4.1c) are substituted into Equation (4.2), the last integral of Equation (4.2) equals zero after integration. If this is the case, then there would not be any relaxation to the nonlinear spring force which is introduced by the fourth integral in Equation (4.2). In other words, the tangential displacement components u'' and v'' do not play any role in restraining the enlargement of the normal displacement component w'', even the ends are completely restricted. Apparently, this is not true. Therefore, the additional terms of Equations (4.1a) and (4.1b) must be introduced at this stage.

The Lagrangian function used in the Hamilton principle is, as it has been described in Section 2.5, the sum of expressions of Equations (2.15) (with negative sign), (2.23) and (2.24). The direct variational operation to Equation (2.16) gives six equations of the generalized coordinates $A_1, A_2, A_3; B_1, B_2$ and C_1. Because of the orthogonality among certain terms of Equation (4.2), A_1 and B_1 are uncoupled with A_2 and B_2, while A_3 is uncoupled with all A_1, A_2, B_1 and B_2. Five of the six equations are algebraic ones; thus, they can be solved simultaneously to express $A_1, A_2, A_3; B_1$ and B_2 in terms of C_1. The last one is a nonlinear differential equation with variable coefficient. By considering the first five equations, this differential equation can be arranged to have C_1 its only argument.

For sinusoidal temperature load, they are

$$(\bar{A}_1)_s = F_4\,(\bar{C}_1)_s \tag{4.3}$$

$$(\bar{B}_1)_s = F_5\,(\bar{C}_1)_s \tag{4.4}$$

$$(\bar{A}_2)_s = F_8\,(\bar{C}_1)_s^2\,\left(\frac{h}{x_1}\right) \tag{4.5}$$

$$(\bar{B}_2)_s = F_9\,(\bar{C}_1)_s^2\,\left(\frac{h}{x_1}\right) \tag{4.6}$$

$$(\bar{A}_3)_s = F_{10}\,(\bar{C}_1)_s^2\,\left(\frac{h}{x_1}\right) \tag{4.7}$$

$$\frac{d^2(\bar{C}_1)_s}{d\bar{\bar{\tau}}^2} - \frac{\Omega_{mn}^2}{\Omega_1^2}\left(1 - \frac{T_0}{T_{cr}}\cos\bar{\bar{\tau}}\right)(\bar{C}_1)_s + \frac{(\eta_1 - \eta_2 - \eta_3)}{\Omega_1^2}(\bar{C}_1)_s^3 = 0 \tag{4.8}$$

in which the bar over the generalized coordinates A_1, A_2, A_3 ; B_1, B_2 and C_1 indicates that these generalized coordinates are nondimensionalized, i.e., $\bar{A}_1 = A_1/h$, $\bar{A}_2 = A_2/h$, $\bar{A}_3 = A_3/h$; $\bar{B}_1 = B_1/h$, $\bar{B}_2 = B_2/h$ and $\bar{C}_1 = C_1/h$.

In general, F_8, F_9 and F_{10} are functions of (ζ_0, θ, m, n), and η_1, η_2 and η_3 are functions of ($\zeta_0, \theta, m, n, \frac{R_1}{h}$). η_1 is the nonlinear force introduced by the first term of u'' and v'' . η_2 is the nonlinear force introduced by the second term of u'' and v'' , while η_3 is the nonlinear force introduced by the third term of u''. They are listed in Appendix I.

For ramp-type thermal loading, the final equations take the following forms

$$(\bar{A}_1)_r = F_4(\bar{C}_1)_r \tag{4.9}$$

$$(\bar{B}_1)_r = F_5(\bar{C}_1)_r \tag{4.10}$$

$$(\bar{A}_2)_r = F_8(\bar{C}_1)_r^2\left(\frac{h}{x_1}\right) \tag{4.11}$$

$$(\bar{B}_2)_r = F_9(\bar{C}_1)_r^2\left(\frac{h}{x_1}\right) \tag{4.12}$$

$$(\bar{A}_3)_r = F_{10}(\bar{C}_1)_r^2\left(\frac{h}{x_1}\right) \tag{4.13}$$

$$\frac{d^2(\bar{C}_1)_r}{d\bar{\tau}^2} + \frac{\Omega_{mn}^2}{\omega^2}\left(1 - \frac{T_1}{T_{cr}} - \frac{T_1}{T_r}\cos\bar{\tau}\right)(\bar{C}_1)_r - \frac{\eta_1-\eta_2-\eta_3}{\omega^2}(\bar{C}_1)_r^3 = 0 \tag{4.14}$$

It is appropriate to point out here that if all nonlinear terms of $(\bar{C}_1)_s$ and $(\bar{C}_1)_r$ are dropped, then the above two sets of equations reduce to the corresponding linear ones. As one may observe, they are exactly the same as those obtained in the preceding chapter [Equations (3.14a), (3.14b) (3.14c); (3.15a), (3.15b) and (3.15c)].

Equations (4.8) and (4.14) are the governing equations for studying the problem of nonlinear dynamic behavior.

4.1.2 Nonlinear vibrations

If terms which include temperature T_0 or T_1 in Equations (4.8) and (4.14) are set to zero, i.e., if the shell is free of any external temperature, then both equations reduce to the following unique form.

$$\frac{d^2\bar{C}_1}{d\tau^2} + \Omega_{mn}^2\bar{C}_1 + (\eta_1-\eta_2-\eta_3)\bar{C}_1^3 = 0 \tag{4.15}$$

Equation (4.15) governs the nonlinear free vibration of a conical shell. The solution of Equation (4.15) can be expressed as

$$\bar{C}_1 = \sum_{i=1}^{\infty} a_i(\cos(i\Omega\tau) + \sin(i\Omega\tau)) \tag{4.16}$$

As a first approximation, $\bar{C}_1$ can be written as

$$\bar{C}_1 = a_1(\cos(\Omega\tau) + \sin(\Omega\tau)) \tag{4.17}$$

Substituting Equation (4.17) into Equation (4.15) and comparing coefficients of corresponding modes after calculation yields

$$1 - \left(\frac{\Omega}{\Omega_{mn}}\right)^2 + \frac{3}{4\Omega_{mn}^2}(\eta_1 - \eta_2 - \eta_3)\,a_1^2 = 0 \tag{4.18}$$

Equation (4.18) gives the relation between the frequency of free vibration Ω and the corresponding vibrating amplitude a_1.

4.1.3 Dynamic stability and response

One may notice that both Equations (4.8) and (4.14) are of the same form as the so-called nonlinear Mathieu differential equation [33]. For the purpose of simplicity, the following Equation (4.19) is used to develop the solution. One just compares Equations (4.8) and (4.14) with Equation (4.19); then the corresponding solutions will be obtained.

$$\frac{d^2\bar{C}_1}{dy^2} + \left(\frac{\Omega_{mn}}{\bar{\Omega}}\right)^2\left[(1 - 2\mu\cos y)\bar{C}_1 + \beta\bar{C}_1^3\right] = 0 \tag{4.19}$$

It has been known, [2], [30], [33] and [34], that the instability regions of the linear solution of Equation (4.19) are located near

$$\bar{\Omega} = 2\Omega_{mn}/\ell \qquad (\ell = 1, 2, \cdots) \tag{4.20}$$

The most dangerous of these regions is the first instability region which has been used in discussing the dynamic stability for the linear case in Chapter 3. Therefore, as a first approximation, the solution of Equation (4.19) will be taken in the following forms which are near the principal (first) instability region [30].

$$\bar{C}_1 = b_1 \cos\frac{\gamma}{2} \tag{4.21a}$$

for the branch adjoining the lower boundary of the instability region, and

$$\bar{C}_1 = c_1 \sin\frac{\gamma}{2} \tag{4.21b}$$

for the branch adjoining the upper boundary of the instability region. In Equation (4.21), b_1 and c_1 are two constant coefficients representing the amplitudes of the normal displacement component of the shell. After substituting Equations (4.21a) and (4.21b) into Equation (4.19), b_1 and c_1 can be solved through the process of comparing coefficients. They are

$$b_1^2 = \frac{4}{3\beta}\left(\frac{\xi^2}{4} - 1 + \mu\right) \tag{4.22a}$$

$$c_1^2 = \frac{4}{3\beta}\left(\frac{\xi^2}{4} - 1 - \mu\right) \tag{4.22b}$$

where $\xi^2 = \frac{\bar{\Omega}}{\Omega_{mn}}$. These expressions coincide with the corresponding relationships for plates [2].

It is of interest to point out that as long as one remembers that the term containing $\cos\frac{\gamma}{2}$ or $\sin\frac{\gamma}{2}$ is the dominant term in the solution, a second approximation of the solution gives exactly the same results for b_1 and c_1 as obtained by the first approximation. As a second approximation, the solution of $\bar{C}_1$ will be taken in the following forms

$$\bar{C}_1 = b_0 + b_1 \cos \frac{y}{2} + b_2 \cos y \qquad (4.23a)$$

$$\bar{C}_1 = c_0 + c_1 \sin \frac{y}{2} + c_2 \sin y \qquad (4.23b)$$

The reason for inclusion of the free terms b_0 and c_0 is self-evident. Indeed, inserting $\cos y$ into the nonlinear part of Equation (4.19), one will arrive at an expression with a constant term of the same order of magnitude as the coefficient of $\cos y$. Inserting Equation (4.23a) into Equation (4.19), and taking $b_1 \gg b_0$, $b_1 \gg b_2$, one will obtain three nonlinear algebraic equations containing b_0, b_1 and b_2 by equaling the coefficients of the free term, $\cos \frac{y}{2}$ and $\cos y$ to zero. These three equations are of the following forms

$$\left(1 + \frac{3}{2}\beta b_1^2\right) b_0 + \left(\frac{3}{4}\beta b_1^2 - \mu\right) b_2 = 0 \qquad (4.24a)$$

$$\left(\frac{3}{2}\beta b_1^2 - 2\mu\right) b_0 + \left(\frac{3}{2}\beta b_1^2 + 1 - \xi^2\right) b_2 = 0 \qquad (4.24b)$$

$$1 - \frac{\xi^2}{4} - \mu + \frac{3}{4}\beta b_1^2 = 0 \qquad (4.24c)$$

Equation (4.24c), as one can notice, is exactly the same as Equation (4.22a). Thus, Equations (4.24a) and (4.24b) give b_0 and b_2 only a trivial solution.

Inserting Equation (4.23b) into Equation (4.19) and making the same simplification $c_1 \gg c_0$, $c_1 \gg c_2$, three nonlinear equations of c_0, c_1, c_2 will be obtained as

$$\left(1 + \frac{3}{2}\beta c_1^2\right) c_0 - \left(\mu + \frac{3}{4}\beta c_1^2\right) c_2 = 0 \qquad (4.25a)$$

$$-\left(2\mu + \frac{3}{2}\beta c_1^2\right) c_0 + \left(1 - \xi^2 + \frac{3}{2}\beta c_1^2\right) c_2 = 0 \qquad (4.25b)$$

$$1 - \frac{\xi^2}{4} + \mu + \frac{3}{4}\beta c_1^2 = 0 \qquad (4.25c)$$

Equation (4.15c) is the same as Equation (4.22b). Thus, Equations (4.25a) and (4.25b) give c_0 and c_2 only a trivial solution.

From Equations (4.24c) and (4.25c), one may plot b_1 and c_1 against the frequency parameter ξ^2 and thus form the so-called response curves in the amplitude-frequency plane. Usually, the absolute value of b_1 and c_1 is used as the ordinate, while ξ^2 is used as the abscissa (See Figs. 9a,b,c). When $\beta = 0$, these response curves reduce to their counterparts of a linear forced vibration (See Fig. 9c). When $\mu = 0$, Equations (4.24c) and (4.25c) become identical. The response curve for $\mu = 0$ is drawn heavier. Comparing Figures 9a,b with Figure 9c, one sees that the response curves in the nonlinear cases could be thought of as arising from those for the linear case by bending the latter to the right for a hard spring and to the left for a soft spring. Also from these two figures, one sees that for the linear vibration the relation between the amplitude and the frequency is conformal, while for the nonlinear case it is not. For certain values of ξ^2, there could be two different values of b_1 or c_1.

Because of the nonconformal relation between the amplitude and the frequency, the so-called jump phenomenon happens. This phenomenon will provide the information of the stability condition of the shell under consideration. Let us imagine an experiment performed in which μ is held constant, while $\bar{\Omega}$ is slowly varied, and the amplitudes b_1 and c_1 of the resulting harmonic vibration are observed. Consider first the case of a hard spring force, $\beta > 0$, and suppose that ξ^2 is rather large at the beginning of the experiment, i.e., by referring to Figure 10a, it is started at point 1 on the curve. As ξ^2 is

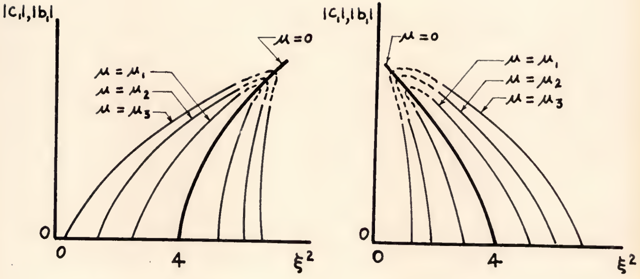

$\beta > 0$ (Hard Spring)

(a)

$\beta < 0$ (Soft Spring)

(b)

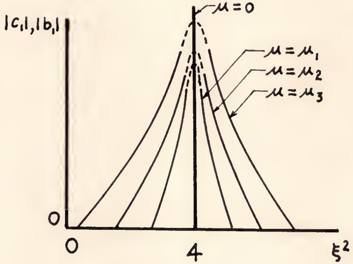

$\beta = 0$ (Linear Case)

(c)

Figure 9. Amplitude-Frequency Diagram

decreased, C_1 immediately jumps to b_1 at point 2, then follows the path through point 3. Upon performing the experiment in the other direction, i.e., starting at point 4 and increasing ξ^2, the amplitude follows the path 4-3-2 to infinity without any jump. In the real case, there are always damping forces in the shell no matter how small they are. Therefore, for the present case, one may imagine that the solution of the amplitude following the path 4-3-2 will jump at a point 5 near infinity to point 6 on the abscissa. The circumstances are quite similar with a soft spring force, but the jumps in amplitude take place in the reverse direction (See Fig. 10b).

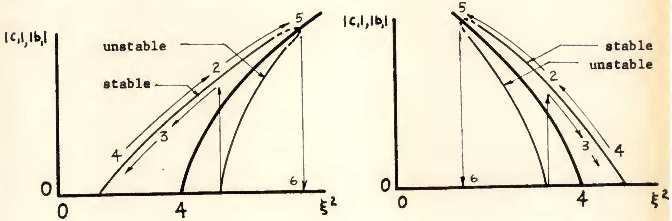

$\beta > 0$

(a)

$\beta < 0$

(b)

Figure 10. Jump Diagram

It seems plausible that the solution corresponding to absolute values of the amplitude and the frequency parameter for those portions of the harmonic response curves which are passed over in jumping from one point to another are unstable solutions. In other words, for the hard spring force, the solution originating at the upper boundary of the instability region is unstable, while for the soft spring force, the solution originating at the lower boundary of the instability region is unstable. This is shown in Figure 10.

In discussing conical shells, one may compare Equations (4.8) and (4.14) with Equation (4.19) to find out their correspondences. For the sinusoidal temperature load, Equations (4.24c) and (4.25c) take the following forms

$$1-\frac{1}{4}\frac{\Omega_1^2}{\Omega_{mn}^2}-\frac{1}{2}\frac{T_0}{T_{cr}}+\frac{3}{4}\left(\frac{1}{\Omega_{mn}^2}\right)(\eta_1-\eta_2-\eta_3)\,b_1^2=0 \tag{4.26a}$$

$$1-\frac{1}{4}\frac{\Omega_1^2}{\Omega_{mn}^2}+\frac{1}{2}\frac{T_0}{T_{cr}}+\frac{3}{4}\left(\frac{1}{\Omega_{mn}^2}\right)(\eta_1-\eta_2-\eta_3)\,c_1^2=0 \tag{4.26b}$$

For the ramp-type temperature load, Equations (4.24c) and (4.25c) take forms as

$$1-\frac{T_1}{T_{cr}}-\frac{1}{4}\frac{\omega^2}{\Omega_{mn}^2}-\frac{1}{2}\frac{T_1}{T_r}+\frac{3}{4}\left(\frac{1}{\Omega_{mn}^2}\right)(\eta_1-\eta_2-\eta_3)\,b_1^2=0 \tag{4.27a}$$

$$1-\frac{T_1}{T_{cr}}-\frac{1}{4}\frac{\omega^2}{\Omega_{mn}^2}+\frac{1}{2}\frac{T_1}{T_r}+\frac{3}{4}\left(\frac{1}{\Omega_{mn}^2}\right)(\eta_1-\eta_2-\eta_3)\,c_1^2=0 \tag{4.27b}$$

The correspondence between coefficients of Equations (4.24c) and (4.25c) and Equations (4.26a), (4.26b); (4.27a), (4.27b) is shown in Table II.

TABLE II

CONVERSION OF COEFFICIENTS OF THE NONLINEAR MATHIEU DIFFERENTIAL EQUATION

		ξ^2	μ	β
Conical Shell	Sinusoidal Temperature Loading	$\left(\frac{\Omega_1}{\Omega_{mn}}\right)^2$	$\frac{1}{2}\frac{T_o}{T_{cr}}$	$\frac{\eta_1-\eta_2-\eta_3}{\Omega_{mn}^2}$
	Ramp-type Temperature Loading	$\left(\frac{\omega}{\Omega_{mn}}\right)^2\left(\frac{T_{cr}}{T_{cr}-T_1}\right)$	$\frac{1}{2}\frac{T_1}{T_r}\left(\frac{T_{cr}}{T_{cr}-T_1}\right)$	$\left(\frac{T_{cr}}{T_{cr}-T_1}\right)\left(\frac{\eta_1-\eta_2-\eta_3}{\Omega_{mn}^2}\right)$
Cylindrical Shell	Sinusoidal Temperature Loading	$\left(\frac{\Omega_1}{\Omega_{mn}^c}\right)^2$	$\frac{1}{2}\frac{T_o}{T_{cr}^c}$	$\frac{\eta_{1c}-\eta_{2c}-\eta_{3c}}{(\Omega_{mn}^c)^2}$
	Ramp-type Temperature Loading	$\left(\frac{\omega_c}{\Omega_{mn}^c}\right)^2\left(\frac{T_{cr}^c}{T_{cr}^c-T_1}\right)$	$\frac{1}{2}\frac{T_1}{T_r^c}\left(\frac{T_{cr}^c}{T_{cr}^c-T_1}\right)$	$\left(\frac{T_{cr}^c}{T_{cr}^c-T_1}\right)\left(\frac{\eta_{1c}-\eta_{2c}-\eta_{3c}}{(\Omega_{mn}^c)^2}\right)$

4.2 Cylindrical Shells

In this section, the scale factor B and the curvature of the shell k_ϕ, appearing in all basic equations of Chapter 2, are expressed by Equations (2.3) and (2.5). The detailed analysis of the cylindrical shell through the procedure stated in Section 2.5 is given in the following sections. Since the general approach is the same as that for a conical shell, certain steps which have been discussed thoroughly in the above section will not be repeated in the present section in detail.

4.2.1 Basic governing nonlinear equations

The prebuckling solutions to the present case are the same as those in Section 3.2.1. All equations in Section 3.2.1 are used for further analysis in the present section.

After buckling, the additional displacement components are assumed as

$$u_c'' = A_{1c}(t)\left[\sin\left(\frac{m\pi x}{L}\right) - (-1)^{\frac{m-1}{2}}\left(\frac{2x}{L}\right)\right]\sin(n\phi) + A_{2c}(t)\sin\left(\frac{2m\pi x}{L}\right)\cos(2n\phi) + A_{3c}(t)\sin\left(\frac{2m\pi x}{L}\right) \tag{4.28a}$$

$$v_c'' = B_{1c}(t)\cos\left(\frac{m\pi x}{L}\right)\cos(n\phi) + B_{2c}(t)\left(\cos\left(\frac{2m\pi x}{L}\right) + 1\right)\sin(2n\phi) \tag{4.28b}$$

$$w_c'' = C_{1c}(t)\cos\left(\frac{m\pi x}{L}\right)\sin(n\phi) \tag{4.28c}$$

The additional terms $A_{2c}(t)\,\mathrm{Sin}\left(\frac{2m\pi x}{L}\right)\mathrm{Cos}(2n\phi)$, $A_{3c}(t)\,\mathrm{Sin}\left(\frac{2m\pi x}{L}\right)$ and $B_{2c}(t)\left(\mathrm{Cos}\left(\frac{2m\pi x}{L}\right)+1\right)\mathrm{Sin}(2n\phi)$ are introduced for the same purpose as explained in the last section, i.e., they are introduced to show the effects of the nonlinear coupling terms of the displacement components in the strain energy expression.

The Lagrangian function used in the Hamilton principle is the sum of expressions of Equations (2.15) (with negative sign), (2.23) and (2.24). The direct variational operation to Equation (2.16) gives six equations of the general coordinates A_{1c}, A_{2c}, A_{3c} ; B_{1c}, B_{2c} and C_{1c}. Through the same arrangement described in Section 4.1.1, the final governing nonlinear differential equations, corresponding to Equations (4.8) and (4.14) for the conical shell, assume the following forms

$$\frac{d^2(\bar{C}_{1c})_s}{d\bar{\bar{\tau}}^2}+\frac{(\Omega^c_{mn})^2}{\Omega_1^2}\left(1-\frac{T_0}{T^c_{cr}}\cos\bar{\bar{\tau}}\right)(\bar{C}_{1c})_s-\frac{\eta_{1c}-\eta_{2c}-\eta_{3c}}{\Omega_1^2}(\bar{C}_{1c})^3_s=0 \quad (4.29)$$

$$\frac{d^2(\bar{C}_{1c})_r}{d\bar{\tau}^2}+\frac{(\Omega^c_{mn})^2}{\omega_c^2}\left(1-\frac{T_1}{T^c_{cr}}-\frac{T_1}{T^c_r}\cos\bar{\tau}\right)(\bar{C}_{1c})_r-\frac{\eta_{1c}-\eta_{2c}-\eta_{3c}}{\omega_c^2}(\bar{C}_{1c})^3_r=0 \quad (4.30)$$

where η_{1c} . η_{2c} and η_{3c} are functions of ($\frac{R}{L}, \frac{R}{h}, m, n$) (See Appendix II). If nonlinear terms in Equations (4.29) and (4.30) were dropped, these two equations also reduce to Equations (3.21) and (3.22) obtained in the preceding chapter.

4.2.2 Nonlinear vibrations

Similar to the conical shell, if temperatures T_0 and T_1 are dropped from Equations (4.29) and (4.30), then these two equations reduce to

$$\frac{d^2\bar{C}_{1c}}{d\tau^2}+(\Omega^c_{mn})^2\,\bar{C}_{1c}+(\eta_{1c}-\eta_{2c}-\eta_{3c})\,\bar{C}_{1c}^{\,3}=0 \quad (4.31)$$

Assuming

$$\bar{C}_{1c} = a_{1c} \cos(\Omega \tau) \qquad (4.32)$$

and substituting Equation (4.32) into Equation (4.31) yields

$$1 - \left(\frac{\Omega}{\Omega^c_{mn}}\right)^2 + \frac{3}{4(\Omega^c_{mn})^2}\,(\eta_{1c} - \eta_{2c} - \eta_{3c})\,a^2_{1c} = 0 \qquad (4.33)$$

Equation (4.33) relates the frequency of the free vibration, Ω, and the corresponding vibrating amplitude a_{1c}.

4.2.3 Dynamic stability and response

Equations (4.29) and (4.30) assume the same form as Equation (4.19). Therefore, they are also governed by the criterion developed in the latter part of Section 4.1.3.

For the sinusoidal temperature load, Equations (4.24c) and (4.25c) take the following forms

$$1 - \frac{1}{4}\left(\frac{\Omega_1}{\Omega^c_{mn}}\right)^2 - \frac{1}{2}\frac{T_0}{T^c_{cr}} + \frac{3}{4}\left(\frac{1}{\Omega^c_{mn}}\right)^2 (\eta_{1c} - \eta_{2c} - \eta_{3c})\, b^2_{1c} = 0 \qquad (4.34a)$$

$$1 - \frac{1}{4}\left(\frac{\Omega_1}{\Omega^c_{mn}}\right)^2 + \frac{1}{2}\frac{T_0}{T^c_{cr}} + \frac{3}{4}\left(\frac{1}{\Omega^c_{mn}}\right)^2 (\eta_{1c} - \eta_{2c} - \eta_{3c})\, c^2_{1c} = 0 \qquad (4.34b)$$

For the ramp-type temperature load, Equations (4.24c) and (4.25c) take forms as

$$1 - \frac{T_1}{T^c_{cr}} - \frac{1}{4}\left(\frac{\omega_c}{\Omega^c_{mn}}\right)^2 - \frac{1}{2}\frac{T_1}{T^c_r} + \frac{3}{4}\left(\frac{1}{\Omega^c_{mn}}\right)^2 (\eta_{1c} - \eta_{2c} - \eta_{3c})\, b^2_{1c} = 0 \qquad (4.35a)$$

$$1 - \frac{T_1}{T^c_{cr}} - \frac{1}{4}\left(\frac{\omega_c}{\Omega^c_{mn}}\right)^2 + \frac{1}{2}\frac{T_1}{T^c_r} + \frac{3}{4}\left(\frac{1}{\Omega^c_{mn}}\right)^2 (\eta_{1c} - \eta_{2c} - \eta_{3c})\, c^2_{1c} = 0 \qquad (4.35b)$$

The correspondence between coefficients of Equations (4.24c), (4.25c) and Equations (4.34a), (4.34b) and (4.35a), (4.35b) is also shown in Table II.

4.3 Numerical Results and Discussions

For additional interest, certain numerical results for both cylindrical and conical shells are calculated through IBM 709 and are plotted into curves for several governing parameters. Values of geometric parameters are chosen to be

$$\frac{\bar{R}}{h} = 500, \quad \frac{\bar{R}}{H} = 0.5, \quad \theta = 10^\circ$$

for a conical shell, and

$$\frac{R}{h} = 500, \quad \frac{R}{L} = 0.5$$

for a cylindrical shell.

The force frequency Ω_1, is chosen to equal $2\Omega_{mn}$ or $3\Omega_{mn}$ (Ω^c_{mn} for cylindrical shells). Poisson's ratio, ν, is taken as 0.3. t_0 is assumed to be $\pi\bar{t}$ for the ramp-type temperature loading, and zero for the Heavyside temperature loading. The governing parameters are picked up to be Ω^2_{mn}, $\alpha(T_{cr})_s$, $\alpha(T_{cr})_r$, αT_r, η and $(\Omega^c_{mn})^2$, $\alpha(T^c_{cr})_s$, $\alpha(T^c_{cr})_r$, αT^c_r, η_c, where $\eta = \eta_1 - \eta_2 - \eta_3$ and $\eta_c = \eta_{1c} - \eta_{2c} - \eta_{3c}$. The subscripts s and r indicate the quantities corresponding to sinusoidal, ramp-type or Heavyside temperature loading. These governing parameters are plotted against the mode numbers m and n through Figures 11 - 20.

The free vibration of a conical shell for several different modes is shown in Figure 21, while the free vibration of a cylindrical shell for several different modes is shown in Figure 22. They are of the same form as the free vibration of a simply supported plate [35]. It is observed from Figures 21 and 22, that under the same value of (Ω/Ω_{mn}), the larger the mode number is, the smaller the vibrating amplitude will be. Also in Figures 21 and 22, it reveals that the additional terms added to the displacement components u'', v'' and u_c'', v'' do influence the vibration to a certain degree. Nevertheless, it seems that the third term of u'' or u_c'' (the symmetric term) does a minor job. So it would be of no harm if it is neglected in the calculation.

From Figures 14 and 20, it has been noticed that the nonlinear spring force η or η_c is always positive. This means that for a moderate shell under the present boundary conditions, the nonlinear effect always causes a hard spring force. Therefore, the solution originating from the upper boundary is always unstable while that originating from the lower boundary is always stable. This is shown in Figures 23 and 24. Figures 23 and 24 also reveal that μ and β are two control parameters of the stability of the shell. The width of the instability region bounded by Equations (4.24c) and (4.25c) is controlled by μ, while the slope of the boundaries is controlled by β. Thus, from Table II combining with Figure 23, one will realize that the higher the temperature gradient T_0 or T_1 is, the more dangerous the stability condition for both conical and cylindrical shells will be.

In Figure 25, the stable and unstable solutions of the conical shell subjected to sinusoidal temperature loading with $m=15$, $n=15$, $T_0 = 50°C$ and $\Omega_1 = 3\Omega_{mn}$ and those subjected to ramp-type or Heavyside temperature loading with $m=9$, $n=17$ and $T_1 = 50°C$ have been depicted. ξ^2, μ and β were found by using Table II and Figures 11 - 15. The points P_1 and P_{11} are the stable and unstable solutions under a sinusoidal temperature loading. Similarly, the points P_2 and P_{22} are stable and unstable solutions under a Heavyside temperature load, and the points P_3 and P_{33} are stable and unstable solutions under a ramp-type temperature loading. By looking at P_2 and P_3 , one comes to the same conclusion that was made for the linear case, i.e., the Heavyside temperature loading is more unfavorable than the ramp-type temperature loading. The stable and unstable solutions of the cylindrical shell can be obtained through the same procedure by using Table II and Figures 16 - 20. The results are similar to those of the conical shell.

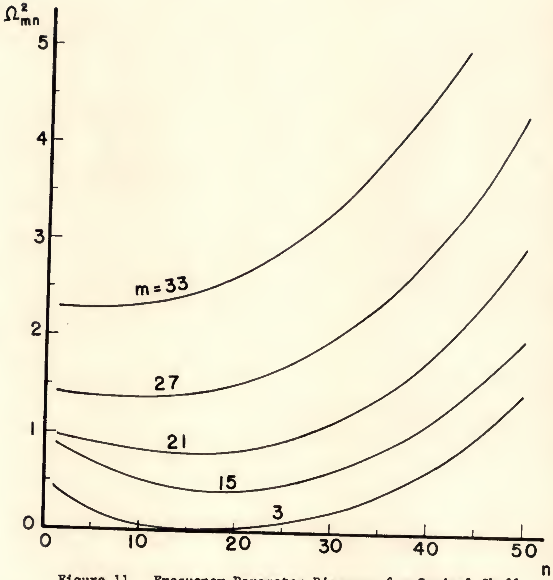

Figure 11. Frequency Parameter Diagram of a Conical Shell ($\bar{R}/H = 0.5$, $\bar{R}/h = 500$, $\theta = 10°$).

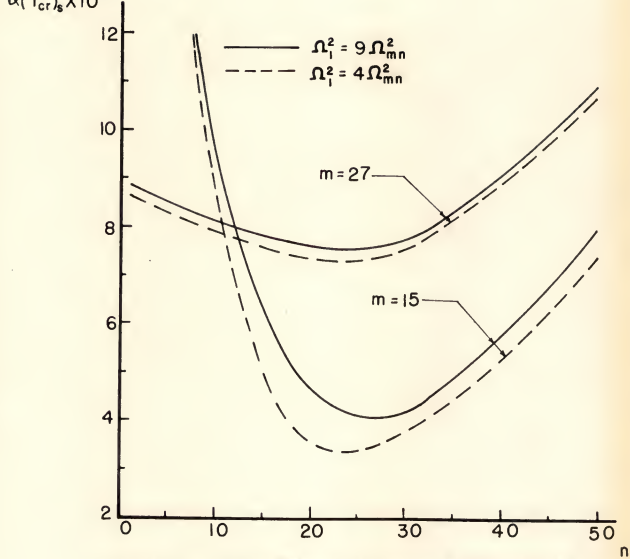

Figure 12. Critical Temperature Diagram of a Conical Shell under Sinusoidal Temperature Loading ($\bar{R}/H = 0.5$, $\bar{R}/h = 500$, $\theta = 10°$, $\Omega_1^2 = 4\Omega_{mn}^2$, $9\Omega_{mn}^2$).

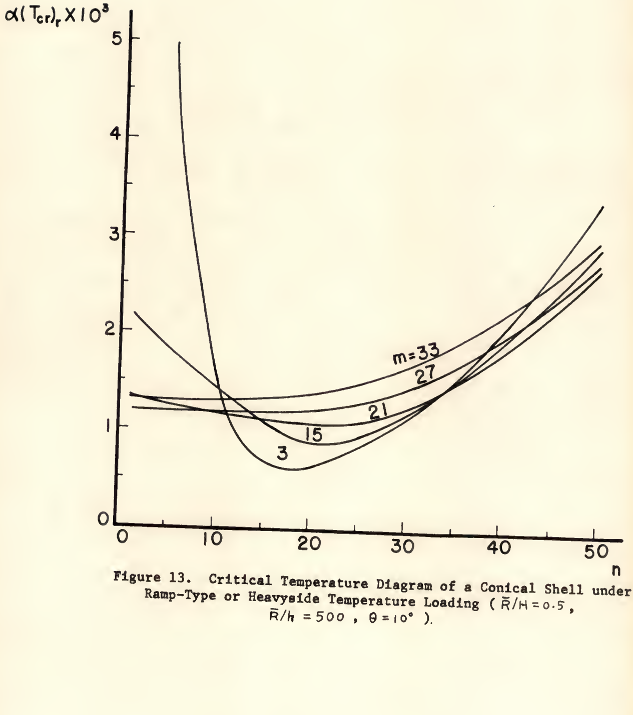

Figure 13. Critical Temperature Diagram of a Conical Shell under Ramp-Type or Heavyside Temperature Loading ($\bar{R}/H = 0.5$, $\bar{R}/h = 500$, $\theta = 10°$).

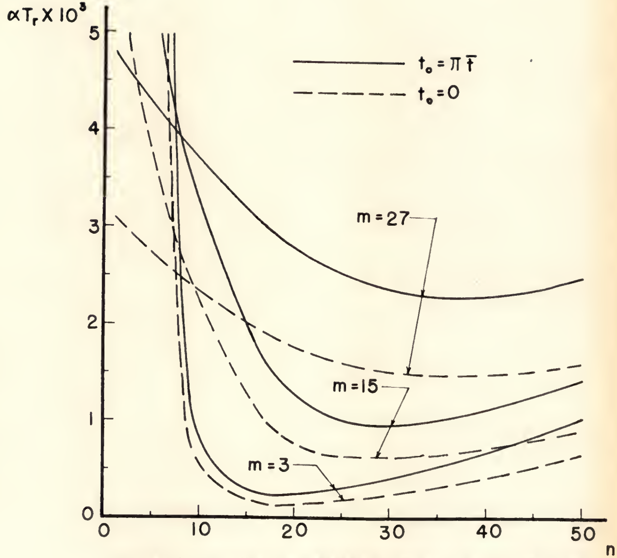

Figure 14. Temperature Parameter Diagram of a Conical Shell under Ramp-Type and Heavyside Temperature Loadings ($\bar{R}/H = 0.5$, $\bar{R}/h = 500$, $\theta = 10°$, $t_o = \pi \bar{\tau}$, 0).

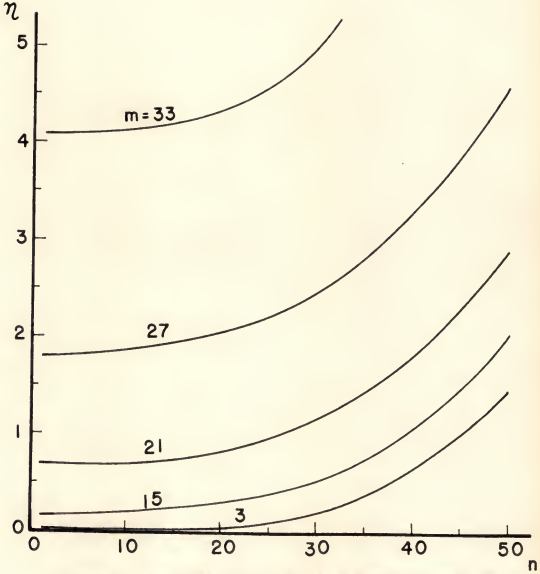

Figure 15. Nonlinear Spring Force Parameter Diagram of a Conical Shell ($\bar{R}/H=0.5$, $\bar{R}/h=500$, $\theta=10°$).

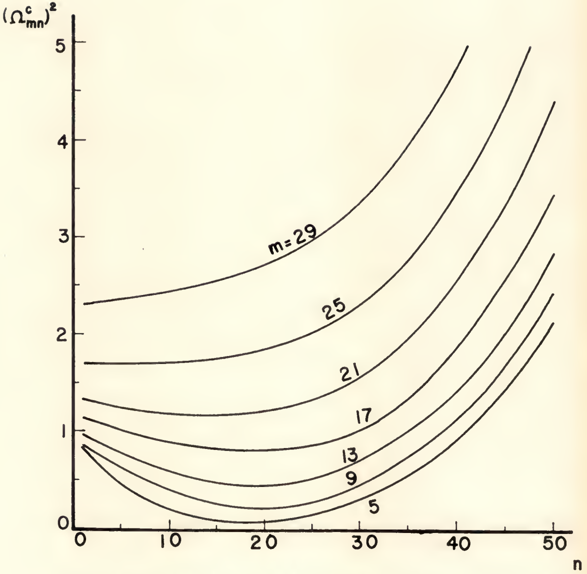

Figure 16. Frequency Parameter Diagram of a Cylindrical Shell ($R/L = 0.5$, $R/h = 500$).

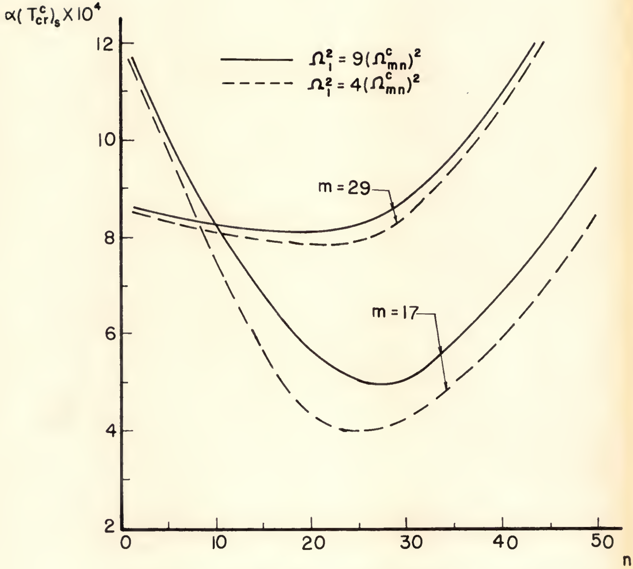

Figure 17. Critical Temperature Diagram of a Cylindrical Shell under Sinusoidal Temperature Loading ($R/L = 0.5$, $R/h = 500$, $\Omega_1^2 = 4(\Omega^c_{mn})^2$, $9(\Omega^c_{mn})^2$).

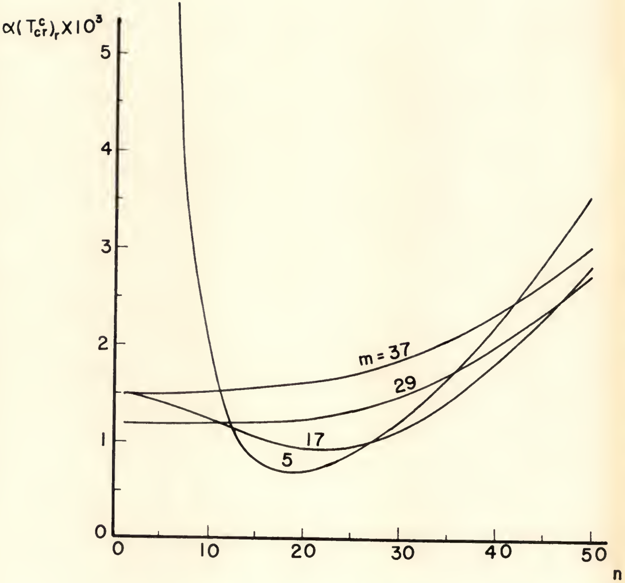

Figure 18. Critical Temperature Diagram of a Cylindrical Shell under Ramp-Type or Heavyside Temperature Loading ($R/L = 0.5$, $R/h = 500$).

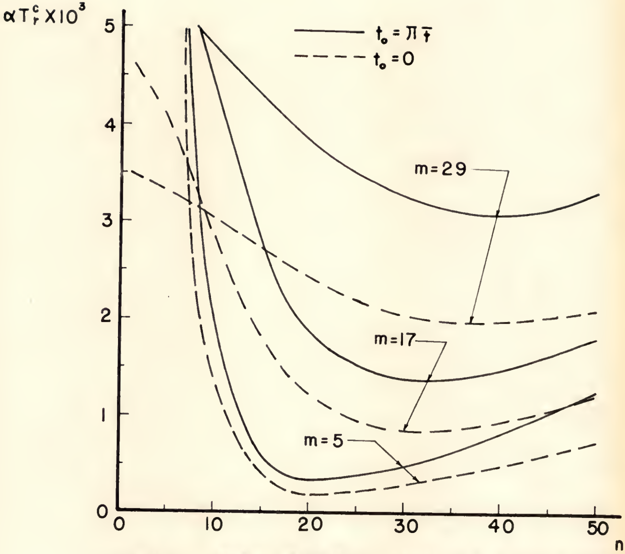

Figure 19. Temperature Parameter Diagram of a Cylindrical Shell under Ramp-Type and Heavyside Temperature Loadings ($R/L = 0.5$, $R/h = 500$, $t_o = \pi\bar{\tau}$, 0).

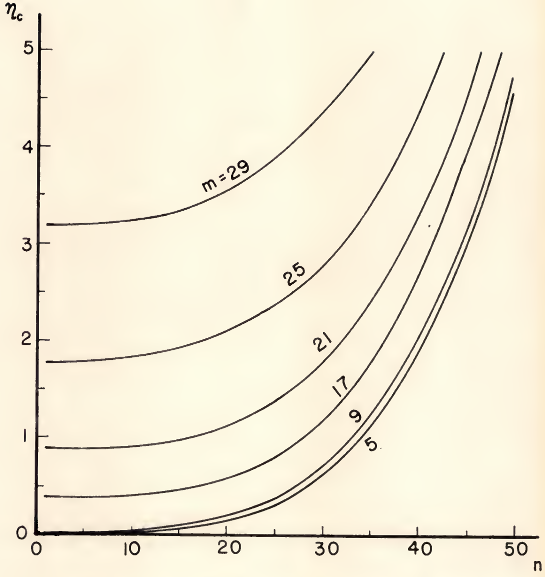

Figure 20. Nonlinear Spring Force Parameter Diagram of a Cylindrical Shell ($R/L=0.5$, $R/h=500$).

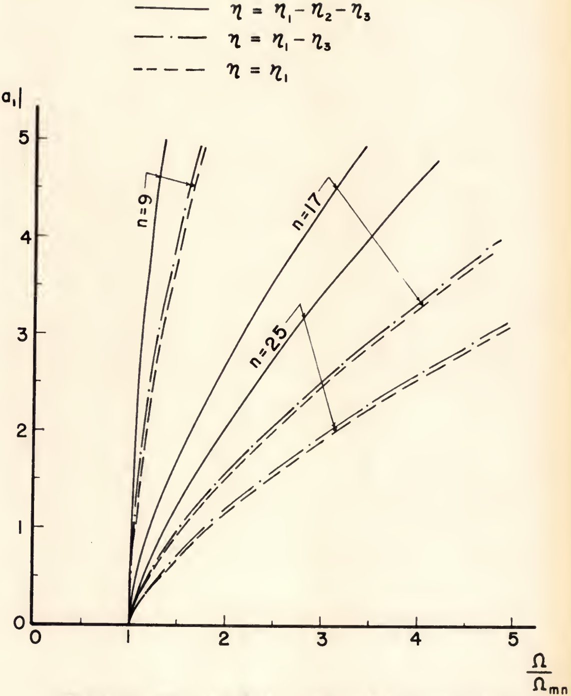

Figure 21. Nonlinear Free Vibration of a Conical Shell ($\bar{R}/H = 0.5$, $\bar{R}/h = 500$, $\theta = 10°$).

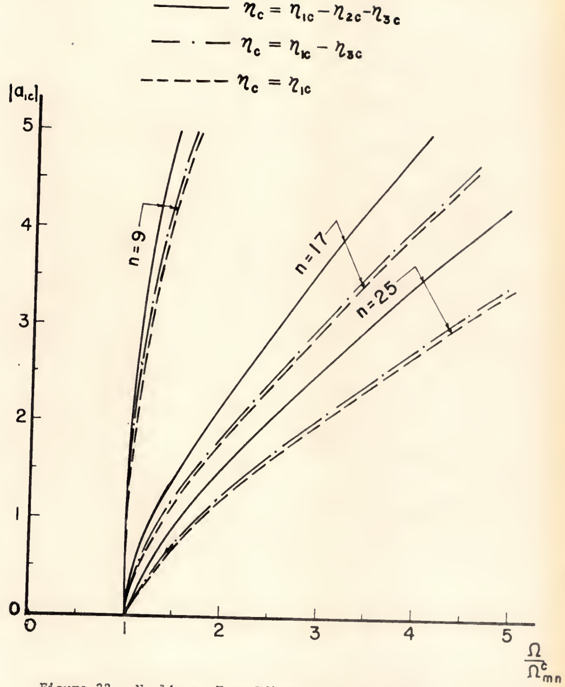

Figure 22. Nonlinear Free Vibration of a Cylindrical Shell ($R/L = 0.5$, $R/h = 500$).

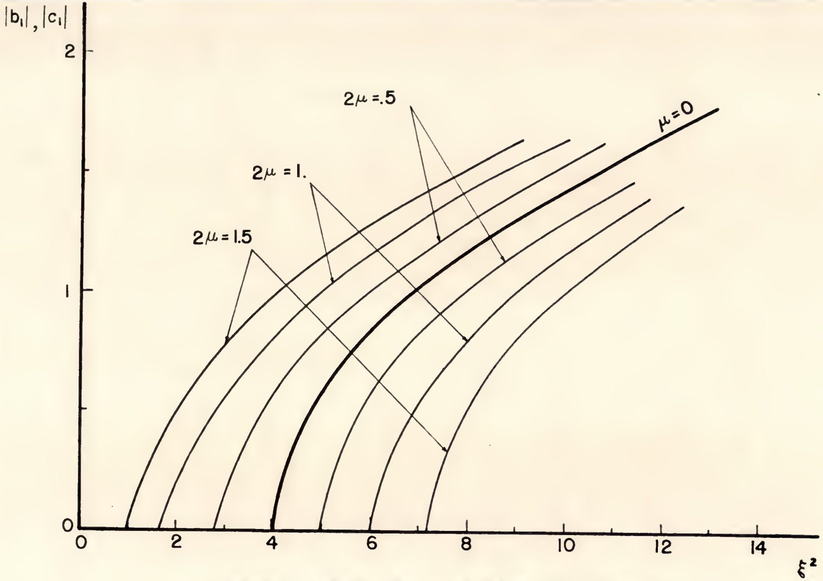

Figure 23. Amplitude-Frequency Diagram with Constant β.

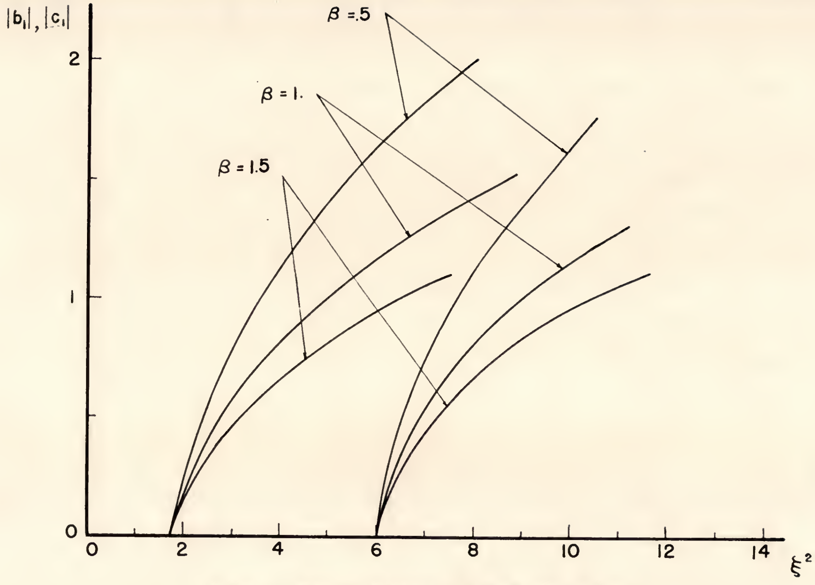

Figure 24. Amplitude-Frequency Diagram with Constant μ.

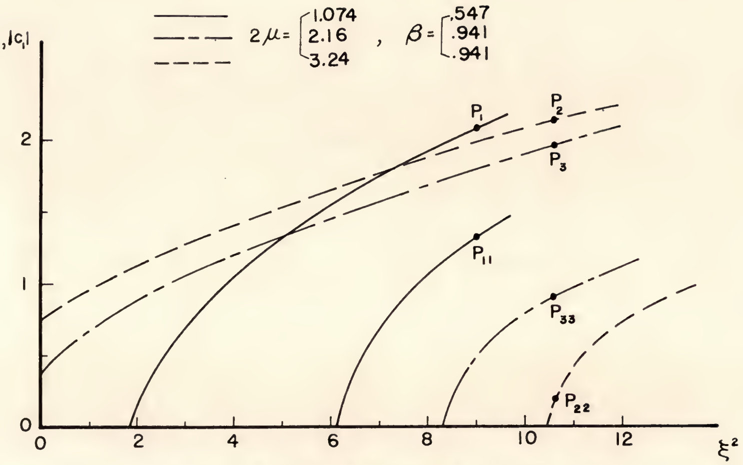

Figure 25. **Amplitude-Frequency Diagram of a Conical Shell**
($\bar{R}/H = 0.5$, $\bar{R}/h = 500$, $\theta = 10°$, $\alpha T_0 = 6.6 \times 10^{-4}$;
$\alpha T_1 = 6.6 \times 10^{-4}$, $\Omega_1 = 3\Omega_{mn}$, $t_0 = 0$, $\pi\bar{t}$)

CHAPTER 5

CONCLUSION

An energy approach, to analyze the dynamic behavior of conical and cylindrical shells under surface temperature load by linear and nonlinear shallow shell theories through steps stated in Chapter 2, is able to find out some characteristics of this kind of problem. For the linear case, it tells us that the essential effects on dynamic stability of conical and cylindrical shells come from the inertia terms of the prior buckling equation of motion as well as the radius-thickness ratio of the shell. Lengths and appex angles are less influential factors in the present problem. Generally speaking, the dynamic stability is more dangerous than the static stability under the proposed boundary and loading conditions. For the nonlinear case, it reveals that additional terms of the tangential displacement components are needed. Otherwise, the nonlinear force calculated would be larger than it actually is. For shells with moderate size, under the present boundary conditions, the nonlinear effect always exercises a hard spring force. Thus, the response solution originating at the upper boundary of the instability region is always unstable, while the response solution originating at the lower boundary of the instability region is always stable.

For both conical and cylindrical shells, the dynamic stability condition becomes more dangerous when the temperature gradient T_0 or T_1

is higher. The free vibration which has infinite modes of frequency is different from the linear free vibration for which the frequency of the vibration equals to the natural frequency of the shell. For sinusoidal temperature loading, higher temperature causes larger response. For ramp-type and Heavyside temperature loadings, the latter causes larger response.

REFERENCES

1. Ziegler, H., "On the Concept of Elastic Stability," Advanced Applied Mechanics, Academic Press, New York, Chap. IV, pp. 351-403, 1956.

2. Bolotin, V. V., The Dynamic Stability of Elastic Systems, Holden-Day, Inc., San Francisco, London, Amsterdam, 1964.

3. Budiansky, B., "Dynamic Buckling of Elastic Structures - Criteria and Estimates," Dynamic Stability of Structures, Proc., International Conference, Northwestern University, Evanston, Illinois, Oct. 18-20, 1965, Pergamon Press, Oxford, London, Edinburgh, New York, Toronto, Sydney, Paris, Braunschweig, pp. 83-106, 1966.

4. Beliaev, N. M., "Stability of Prismatic Rods Subjected to Variable Longitudinal Forces," Collection of Papers: Inzhenernye Sooruzheniia i Stroitel'naia Mechanika, Put', Leningrad, pp. 149-167, 1924.

5. Krylov, N. M. and Bogoliubov, N. N., "Calculations of the Vibrations of Frame Construction with the Consideration of Normal Forces and with the Help of the Methods of Nonlinear Mechanics," Collection of Papers: Issledovanie Kolebanii Konstruksii, ONTI, Kharkov, Kiev, pp. 4-24, 1935.

6. Lubkin, S. and Stoker, J. J., "Stability of Columns and Strings under Periodically Varying Forces," Quart. Appl. Math., Vol. 1, pp. 215-236, 1943.

7. Hoff, N. J., "Buckling and Stability," J. Royal Aeronautical Soc., Vol. 58, pp. 3-52, 1954.

8. Wood, J. D. and Koval, L. R., "Buckling of Cylindrical Shells under Dynamic Loads," AIAA J., Vol. 1, No. 11, pp. 2576-2582, 1963.

9. Donnell, L. H., "Stability of Thin-walled Tubes under Torsion," NACA Report No. 479, 1933.

10. Yao, J. C., "Dynamic Stability of Cylindrical Shells under Static and Periodic Axial and Radial Loads," AIAA J., Vol. 1, No. 6, pp. 1391-1396, 1963.

11. Goodier, J. N. and McIvor, I. K., "The Elastic Cylindrical Shell under Nearly Uniform Radial Impulse," J. Appl. Mech., Vol. 31, Series E, No. 2, pp. 259-266, June, 1964.

12. Bieniek, M. P., Fan, T. C. and Lackman, L. M., "Dynamic Stability of Cylindrical Shells," AIAA J., Vol. 4, No. 3, pp. 495-500, 1966.

13. Bolotin, V. V., "The Stability of Thin Spherical Shells under the Action of a Periodic Force," Collection of Papers: Raschety na Prochnost', Vol. 2, Mashgiz, Moscow, pp. 302-312, 1958.

14. Vol'mir, A. S., "On the Stability of Dynamically Loaded Cylindrical Shells," Soviet Physics-Doklady, Vol. 123, No. 5, pp. 1287-1289, 1958.

15. Agamirov, V. L. and Vol'mir, A. S., "Behaviour of Cylindrical Shells under Dynamic Loading by Hydrostatic Pressure or by Axial Compression," ARS J. Suppl., pp. 98, Jan., 1961, Translated from Bull. Acad. Sci., SSSR, Div. Tech. Sci., Mechanics and Machine Construction, No. 3, pp. 78-83, 1959.

16. Mishenkov, G. V., "On the Dynamic Stability of Shallow Elastic Shells," Inzhenernyi Zhurnal, Vol. I, pp. 112-181, 1961.

17. Cummings, B. E., "Some Nonlinear Vibration and Response Problems of Cylindrical Panels and Shells," Grad. Aeronau. Lab., CIT, Pasadena, Calif., June, 1962.

18. Ho, F. H. and Nash, W. A., "Transitional Instability of Spherical Shells under Dynamic Loadings," Univ. of Fla., 1964 (Dissertation).

19. Wilder, J. A. and Nash, W. A., "Nonlinear Response of a Thin Conical Shell to Dynamically Applied Axial Force," Univ. of Fla., 1965 (Dissertation).

20. Reissner, E., "Transverse Vibrations of Elastic Shells," Q. Appl. Meth., Vol. 13, pp. 169-176, 1955.

21. Boley, B. A., "Thermally Induced Vibrations of Beams," J. of the Aeronau. Sci., Vol. 23, pp. 179-181, 1956.

22. Boley, B. A. and Barber, A. D., "Dynamic Response of Beams and Plates to Rapid Heating," J. Appl. Mech., Vol. 24, pp. 413-416, 1957.

23. Kraus, H., "Thermally Induced Vibrations of Thin Nonshallow Spherical Shells," AIAA J., Vol. 4, No. 11, pp. 500-505, 1966.

24. Lu, S. Y. and Sun, C. L., "Vibrations of Thin Conical Shells Subjected to Sudden Heating," J. of Aircraft, Vol. 4, No. 1, pp. 11-15, Jan.-Feb., 1967.

25. Hoff, N. J., "Buckling of Thin Cylindrical Shells under Hoop Stresses Varying in Axial Direction," J. Appl. Mech., pp. 405-412, Sept., 1957.

26. Sunakawa, M., "Deformation and Buckling of Cylindrical Shells Subjected to Heating," Report No. 370, Aeronau. Research Institute, Univ. of Tokyo, July, 1962.

27. Huang, P. C. and Van Der Maas, C. J., "Large-Deflection Analysis of Buckled Plates under Thermal Effects," The Martin Company, Research Report RR-8, Jan., 1959.

28. Boley, B. A. and Weiner, T. H., Theory of Thermal Stresses, John Wiley and Sons, Inc., New York, London, 1960.

29. Hoff, N. J., Chao, C. C. and Madsen, W. A., "Buckling of Thin-walled Circular Cylindrical Shell Heated along an Axial Strip," J. of Appl. Mech., pp. 253-258, June, 1964.

30. Stoker, J. J., Nonlinear Vibrations, Interscience Publishers, Inc., New York, 1961.

31. Langhaar, H. L., Energy Methods in Applied Mechanics, John Wiley and Sons, Inc., New York, London, 1962.

32. Mushtari, Kh. M. and Sachenkov, A. V., "Stability of Cylindrical and Conical Shells of Circular Cross Section, with Simultaneous Action of Axial Compression and External Normal Pressure," NACA TM 1433, 1958.

33. Minorsky, N., Nonlinear Oscillations, D. Van Nostrand Company, Inc., Princeton, New Jersey, 1962.

34. Ogibalov, P. M., "Dynamics and Strength of Shells," NASA TT F-284, Translated from Russian, pp. 196-220, 1966.

35. Yu, Y. Y. and Lai, J. L., "Influence of Transverse Shear and Edge Condition on Nonlinear Vibration and Dynamic Buckling of Homogeneous and Sandwich Plates," J. of Appl. Mech., Vol. 33, No. 4, pp. 934-936, Dec., 1966.

APPENDICES

APPENDIX I

FORMULATIONS OF THE CONICAL SHELL

$$I = \pi/\zeta_0, \quad S\theta = \sin\theta, \quad K\theta = \cot\theta$$

$$E_1 = \exp(\zeta_0) - 1, \quad E_2 = \exp(2\lambda\zeta_0) - 1, \quad E_3 = \exp(\lambda\zeta_0) + 1,$$

$$E_4 = \exp[(1+\lambda)\zeta_0] + 1, \quad E_5 = \exp[2(\lambda-1)\zeta_0] - 1, \quad E_6 = \exp[(2\lambda-1)\zeta_0] - 1,$$

$$E_7 = \exp[(3\lambda-1)\zeta_0] + 1, \quad E_8 = \exp[(2+\lambda)\zeta_0] + 1, \quad E_9 = \exp[2(1+\lambda)\zeta_0],$$

$$E_{10} = 1 - \exp[(4\lambda-2)\zeta_0],$$

$$P = 1 + 16I^2, \quad P_1 = I^2 + \lambda^2, \quad P_{11} = I^2 + (1+\lambda)^2, \quad P_{111} = I^2 + (1-\lambda)^2,$$

$$P_2 = 9I^2 + \lambda^2, \quad P_{22} = 9I^2 + (1+\lambda)^2, \quad P_{222} = 9I^2 + (1-\lambda)^2,$$

$$\Delta_1 = (2I^2 + 1/2)\zeta_0, \quad \Delta_2 = 8I(1+4I)E_1 P^{-1}, \quad \Delta_3 = I^2 E_2/(4\lambda P_1),$$

$$\Delta_4 = (1/P_2 - 1/P_1)E_3\lambda, \quad \Delta_5 = (1/P_{22} - 1/P_{11})E_4(1+\lambda)/(2I),$$

$$\Delta_6 = 2(3/P_2 - 1/P_1)E_3 I^2, \quad \Delta_7 = (3/P_{22} - 1/P_{11})E_4 I,$$

$$\Delta_8 = I^2 + 3\lambda^2, \quad \Delta_9 = I^2 - \lambda^2, \quad \Delta_{10} = -2IE_4/P_{11},$$

$$B_{11} = I^2(E_9 - 1)/\{2(1+\lambda)[(1+\lambda)^2 + I^2]\},$$

$$B_{22} = \{(\Delta_8\Delta_9 + 4\lambda^3) - 4\lambda(\lambda-1)[2(1-\lambda)^2 + I^2)]\} I^2[4(\lambda-1)P_{111}]^{-1} + 2\lambda^2 I^2(\lambda-1)/P_{111},$$

$$H_{RR} = (h/R_1)^2(S\theta)^2/12, \quad \omega^2 = [2(K\theta)^2\Delta_3 - (K\theta)^2(\Delta_4 + \nu\Delta_6)^2/(2\Delta_1) + 2B_{22}H_{RR}](S\theta)^2/B_{11},$$

$$F_1 = K\theta(\Delta_4 + \nu\Delta_6)/(2\Delta_1),$$

$$F_2 = K\theta(1+\nu)[(\Delta_5 + \nu)(\Delta_7 + \Delta_5) + \Delta_{10} - \Delta_2(\Delta_4 + \nu\Delta_6)/(2\Delta_1)]R_1 S\theta/B_{11},$$

$$F_3 = -(1+\nu)\Delta_2 R_1/(2\Delta_1 S\theta)$$

$$m_1 = mI, \quad n_1 = n/S\theta,$$

$$G_1 = \zeta_0(4m_1^2 + \lambda n_1^2 + 1)/2, \quad G_2 = m_1^2/(\lambda^2 + m_1^2),$$

$$G_3 = 3m_1^2/(\lambda^2 + 9m_1^2), \quad G_4 = G_2 E_2/(4\lambda),$$

$$G_5 = [\lambda/(\lambda^2 + 9m_1^2) - \lambda/(\lambda^2 + m_1^2)]E_3, \quad G_6 = 2(G_3 - G_2)E_3$$

$$G_7 = \lambda(1-\lambda)G_2 E_2/2, \quad G_8 = \lambda m_1^2(2\lambda^2 + m_1^2)E_2/[4\lambda(\lambda^2 + m_1^2)],$$

$G_9 = -\lambda n_1 (G_3 + G_2) E_3, \quad G_{10} = [(1+\lambda-\lambda^2) G_5 + \nu G_6] n_1 + G_9,$

$G_{11} = K\theta (G_5 + \nu G_6), \quad G_{12} = 2(n_1^2 G_4 + G_7 + G_8),$

$G_{13} = 2K\theta n_1 G_4, \quad G_{14} = \{ m_1^2 (m_1^2 + n_1^2)^2 E_5 / [2(\lambda-1)((1-\lambda)^2 + m_1^2)] \} H_{RR},$

$G_{15} = 4\zeta_0 (m_1^2 + \lambda n_1^2), \quad G_{16} = 4 n_1 m_1 (1+\nu)(E_3 - 2)/(1-\nu),$

$G_{17} = 2[3n_1^2/\lambda + m_1^2](E_3 - 2), \quad G_{18} = -m_1 (m_1^2 + n_1^2) E_5 / (4 - 8\lambda),$

$G_{19} = [n_1 (3n_1^2 + (1-2\nu) m_1^2)](E_7 - 2)/(12\lambda - 4),$

$F_4 = [G_{11}(2G_1 G_{12} - G_{10}^2) - G_{10}(2G_1 G_{13} - G_{11} G_{10})] / [2G_1 (2G_1 G_{12} - G_{10}^2)],$

$F_5 = (2G_1 G_{13} - G_{11} G_{10}) / (2G_1 G_{12} - G_{10}^2),$

$F_8 = (G_{19} G_{16} - G_{18} G_{17}) / (G_{15} G_{17} - G_{16}^2),$

$F_9 = (G_{16} G_{18} - G_{15} G_{19}) / (G_{15} G_{17} - G_{16}^2),$

$F_{10} = [m_1 (\nu n_1^2 - m_1^2)] E_5 / [16 \zeta_0 m_1^2 (2\lambda - 1)],$

$\Omega_{mn}^2 = [2(K\theta)^2 G_4 + G_{14} - 2G_4 n_1 F_5 K\theta - (G_5 + \nu G_6) K\theta F_4](S\theta)^2 / B_{11},$

$\eta_1 = (h/R_1)^2 (9m_1^4 + 9n_1^4 + 2m_1^2 n_1^2) E_{10} (S\theta)^4 / [256(\frac{1}{2} - \lambda) B_{11}],$

$\eta_2 = (h/R_1)^2 (G_{18} F_8 + G_{18} F_9)(S\theta)^4 / B_{11},$

$\eta_3 = (h/R_1)^2 (\nu n_1^2 - m_1^2)^2 E_5^2 (S\theta)^4 / [128 \zeta_0 (\frac{1}{2} - \lambda)^2 B_{11}],$

$(Q'_w)_{st} = F_2 \alpha T_1 / \omega^2,$

$Q'_3 = [(Q'_w)_{st} S\theta] / (R_1 T_1 \cos \bar{\tau}),$ **for ramp-type**

$Q'_3 = [(Q'_w)_s S\theta] / (R_1 T_0 \cos \bar{\bar{\tau}}),$ **for sinusoidal type**

$Q'_1 = F_1 Q'_3 + F_3 \alpha S\theta / R_1,$

$G_{20} = 2I[(\lambda - 1/2)^2 + I^2]^{-1}, \quad G_{21} = -2\nu G_{20} Q'_1 E_6,$

$G_{22} = I[(3\lambda - 1)^2 + I^2]^{-1}, \quad G_{23} = K\theta Q'_3 G_{22} E_7, \quad G_{24} = 2I(\lambda^2 + I^2),$

$G_{25} = -\alpha [2\nu G_{24} I^{-1} + \lambda^{-1}] E (1-\lambda), \quad G_{26} = -[\nu^2 + 4(m_1 + I)^2]^{-1},$

$G_{27} = -[\nu^2 + 4(m_1 - I)^2]^{-1}, \quad G_{28} = 2Q'_1 \nu I E_6 [(2+m) G_{26} + (2-m) G_{27}],$

$G_{29} = \{[I + 2m_1]/[(3\lambda - 1)^2 + (I + 2m_1)^2]\} + (I - 2m_1)[(3\lambda - 1)^2 + (I - 2m_1)^2]^{-1},$

$G_{30} = K\theta Q'_3 G_{29} E_7, \quad G_{31} = I[\lambda^2 + (I + m_1)^2]^{-1}, \quad G_{32} = I[\lambda^2 + (I - m_1)^2]^{-1},$

$G_{33} = \alpha(1-\lambda)\{[(\lambda - (1-\lambda)(1+m)) G_{31} + (\lambda - (1-\lambda)(1-m)) G_{32}] I^{-1} - 2\lambda(\lambda^2 + m_1^2)^{-1}\} E_2.$

$$G_{34} = [(\lambda - 1/2)^2 + (I + m_1)^2]^{-1}, \qquad G_{35} = [(\lambda - 1/2)^2 + (m_1 - I)^2]^{-1},$$

$$G_{37} = (3\lambda - 1)\{[(3\lambda-1)^2 + (I + 2m_1)^2]^{-1} - [(3\lambda-1)^2 + (I - 2m_1)^2]^{-1}\},$$

$$G_{36} = -Q_1' E_6 \{[(m+1)I^2 - \nu^2/4]\, G_{34} + [(m-1)I^2 + \nu^2/4]\, G_{35}\},$$

$$G_{38} = K\theta\, Q_3' G_{37} E_7,$$

$$G_{39} = -\alpha[(1-\lambda)/IE_2]\{[I(m+1) + (1-\lambda)\lambda I^{-1}]\, G_{31} +$$

$$+ [I(m_1 - 1) - \lambda(1-\lambda)I^{-1}]\, G_{32} - 2m_1 I(\lambda^2 + m_1^2)^{-1}\}^{-1},$$

$$G_{40} = -Q_1' E_6 (1 + \nu^2)\, G_{20}, \qquad G_{41} = -\alpha[(1-\lambda)/IE_2]\{(1+\nu^2)\, G_{24} + I\lambda^{-1}\}^{-1},$$

$$G_{42} = 2I[(2\lambda-1)^2 + 4(I + m_1)^2]^{-1}, \qquad G_{43} = 2I[(2\lambda-1)^2 + 4(I - m_1)^2]^{-1},$$

$$G_{44} = Q_1' E_6 \{[(1+m) - \nu^2]\, G_{42} + [(1-m) - \nu^2]\, G_{43}\},$$

$$G_{45} = \alpha[(1-\lambda)/IE_2]\{[-(1+\nu)(1+m)/2 + \nu\lambda]\, G_{31} +$$

$$+ [-(1+\nu)(1-m)/2 + \nu\lambda]\, G_{32} - 2\lambda I/(\lambda^2 + m_1^2)\}^{-1},$$

$$T_{cr} = -\Omega_{mn}^2 B_{11}\{[(G_{21} - \nu G_{23} + G_{25})(\lambda^2 + m_1^2) + (G_{28} - \nu G_{30} + G_{33})(m_1^2 - \lambda^2)/2 +$$

$$+ (G_{36} - \nu G_{38} + G_{39})\lambda m_1 + [(G_{40} - G_{23} + G_{41}) + (G_{44} - G_{30} + G_{45})/2]\, n_1^2](S\theta)^2\}^{-1},$$

$$Q_{33}' = -(F_2/\omega^3)(\bar{t}/t_0)[2 - 2\cos(\omega t_0/\bar{t})]^{1/2}\, \alpha S\theta/R_1,$$

$$Q_{11}' = K\theta\, Q_{33}'(\Delta_4 + \nu\Delta_6)/(2\Delta_1),$$

$$G_{46} = -2\nu G_{20} Q_{11}' E_6, \qquad G_{47} = K\theta\, Q_{33}' G_{22} E_7, \qquad G_{48} = Q_{11}' G_{28}/Q_1',$$

$$G_{49} = -Q_{11}' G_{36}/Q_1', \qquad G_{50} = K\theta\, Q_{33}' G_{29} E_7, \qquad G_{51} = K\theta\, Q_{33}' G_{37} E_7$$

$$G_{52} = -Q_{11}' G_{40}/Q_1', \qquad G_{53} = Q_{11}' G_{44}/Q_1',$$

$$T_r = -\Omega_{mn}^2 B_{11}\{[(G_{46} - \nu G_{47})(\lambda^2 + m_1^2) + (G_{48} - \nu G_{50})(m_1^2 - \lambda^2)/2 +$$

$$+ (G_{49} - \nu G_{51})\lambda m_1 + [(G_{52} - G_{47}) + (G_{53} - G_{50})/2]\, n_1^2](S\theta)^2\}^{-1}.$$

APPENDIX II

FORMULATIONS OF THE CYLINDRICAL SHELL

$$F_6 = \nu L/m\pi R, \quad F_7 = -4(1+\nu)R/\pi,$$

$$\omega_c^2 = 1-\nu^2+(h/R)^2(R/L)^4\pi^4/12+(8\nu^2/\pi^2),$$

$$\bar{m} = m\pi/L,$$

$$HRP = (h/R)^2(\bar{m}^2R^2+n^2)^2/12,$$

$$\Lambda = \nu(\bar{m}^2L^2-8)R/(\bar{m}L^2),$$

$$\Lambda_1 = n^2+\lambda\bar{m}^2R^2,$$

$$\Lambda_2 = [(1+\nu)/2\nu]\,n\Lambda,$$

$$\Lambda_3 = \bar{m}^2R^2-(8R^2/L^2)+5(1-\nu)n^2/6-[(8(1-\nu)n^2)/(\bar{m}^2L^2)],$$

$$\Lambda_4 = 4\bar{m}^2R^2+4\lambda n^2,$$

$$\Lambda_5 = 2(1+\nu)n\bar{m}R,$$

$$\Lambda_6 = [\bar{m}^2R^2\lambda+3n^2]4,$$

$$\Lambda_7 = \bar{m}R(\bar{m}^2R^2+n^2)/4,$$

$$\Lambda_8 = n[3n^2+(1-2\nu)\bar{m}^2R^2]/4,$$

$$\overline{AA} = \Lambda\Lambda_1-n\Lambda_2, \quad \overline{BB} = \Lambda_3\Lambda_1-\Lambda_2^2, \quad \overline{CC} = n\Lambda_3-\Lambda\Lambda_2,$$

$$(\Omega_{mn}^c)^2 = [1+HRP-(n\overline{CC}+\Lambda\overline{AA})/\overline{BB}],$$

$$\eta_{1c} = (h/R)^2(9\bar{m}^4R^4+9n^4+2\bar{m}^2n^2R^2)/32,$$

$$\eta_{2c} = 2(h/R)^2(\Lambda_7^2\Lambda_6-2\Lambda_5\Lambda_7\Lambda_8+\Lambda_4\Lambda_8^2)/(\Lambda_4\Lambda_6-\Lambda_5^2),$$

$$\eta_{3c} = (h/R)^2(\nu n^2-\bar{m}^2R^2)^2/16,$$

$$\left.\begin{aligned} G_{60} &= -[\alpha(1+\nu)-(2\nu/\pi)F_7\alpha/(R(\omega_c^2-\Omega_1^2))]\,\bar{m}^2R^2, \\ G_{61} &= -[\alpha(1+\nu)-2[(4m^2-\nu^2)/(4m^2-1)]F_7\alpha/[\pi R(\omega_c^2-\Omega_1^2)]]\,n^2, \end{aligned}\right\} \text{for sinusoidal load}$$

$$\left.\begin{aligned} G_{60} &= -[\alpha(1+\nu)-(2\nu/\pi)F_7\alpha/(R\omega_c^2)]\,\bar{m}^2R^2, \\ G_{61} &= -[\alpha(1+\nu)-2[(4m^2-\nu^2)/(4m^2-1)]F_7\alpha/[\pi R\omega_c^2]]\,n^2, \end{aligned}\right\} \text{for ramp-type load}$$

$$T_{cr}^{c} = -\left[(\Omega_{mn}^{c})^{2}/(G_{60}+G_{61})\right]$$

$$G_{63} = (2\nu/\pi)F_{7}\alpha(\bar{t}/\omega_{c}t_{0})[2-2\cos(\omega_{c}t_{0}/\bar{t})]^{1/2}\bar{m}^{2}R^{2}/(R\omega_{c}^{2}),$$

$$G_{64} = [(4m^{2}-\nu^{2})/(4m^{2}-1)](G_{63}/\nu)(n^{2}/(\bar{m}^{2}R^{2})),$$

$$T_{r}^{c} = \left[(\Omega_{mn}^{c})^{2}/(G_{63}+G_{64})\right].$$

APPENDIX III

FLOW DIAGRAM OF COMPUTER COMPUTATIONS

CONICAL SHELLS

SINUSOIDAL TEMPERATURE

RAMP-TYPE TEMPERATURE

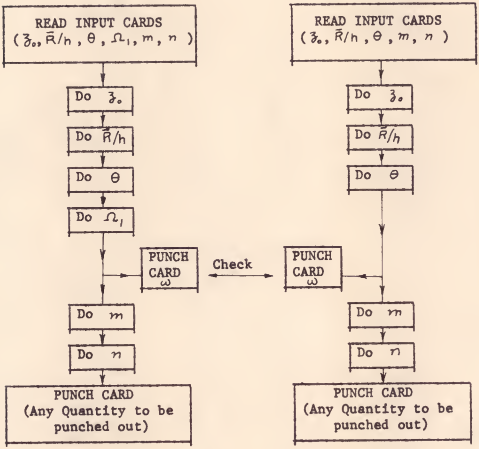
READ INPUT CARDS
(ζ_0, $\bar{R}/h$, θ , Ω_1, m, n)
Do ζ_0
Do $\bar{R}/h$
Do θ
Do Ω_1
PUNCH CARD ω
Check
PUNCH CARD ω
Do m
Do n
PUNCH CARD (Any Quantity to be punched out)
READ INPUT CARDS
(ζ_0, $\bar{R}/h$, θ , m, n)
Do ζ_0
Do $\bar{R}/h$
Do θ
Do m
Do n
PUNCH CARD (Any Quantity to be punched out)

FOR CYLINDRICAL SHELLS, THE PROCEDURE IS THE SAME EXCEPT ζ_0, $\bar{R}/h$ AND ω ARE REPLACED BY R/L , R/h AND ω_c AND THE DO STATEMENT FOR θ IS DROPPED.

BIOGRAPHICAL SKETCH

The author was born on May 21, 1935, in Yangchow, a historical city in the eastern coastal province Kiangsu of China. He finished his elementary school education in Khchiang, China. In 1948, he went to Taipei, Taiwan, and there he completed his high school education in the Subordinate Middle School of Taiwan Normal University in 1953. His first degree, a Bachelor of Science degree in Civil Engineering, was received in 1957, from the National Taiwan University at Taipei. Then he served two years in the Air Force of the Republic of China. In 1963, he received his second degree, a Master of Science degree in Civil Engineering from the same university stated above.

He came to this continent in September, 1963. At first, he studied at the McMaster University in Hamilton, Ontario, Canada, majoring in engineering mechanics. Later in September, 1964, he came to the University of Florida registered as a graduate student in the Department of Engineering Science and Mechanics. He became a Ph.D. degree candidate in February, 1966. His first publication after his arrival in this country was published in January, 1967, together with his adviser, Dr. S. Y. Lu of this university.

This dissertation was prepared under the direction of the chairman of the candidate's supervisory committee and has been approved by all members of that committee. It was submitted to the Dean of the College of Engineering and to the Graduate Council, and was approved as partial fulfillment of the requirements for the degree of Doctor of Philosophy.

August, 1967

Dean, College of Engineering

Dean, Graduate School

Supervisory Committee:

S. Y. Lu
Chairman

W A Nash

R. G. Blake